General phase spaces: from discrete variables to rotor and continuum limits

Victor V. Albert,[1, *] Saverio Pascazio,[2] and Michel H. Devoret[3, †]

[1] *Yale Quantum Institute, Yale University, New Haven, Connecticut 06520, USA*
[2] *Dipartimento di Fisica and MECENAS, Università di Bari, I-70126 Bari, Italy*
Istituto Nazionale di Ottica (INO-CNR), I-50125 Firenze, Italy
INFN, Sezione di Bari, I-70126 Bari, Italy
[3] *Department of Applied Physics, Yale University, New Haven, Connecticut 06520, USA*

We provide a basic introduction to discrete-variable, rotor, and continuous-variable quantum phase spaces, explaining how the latter two can be understood as limiting cases of the first. We extend the limit-taking procedures used to travel between phase spaces to a general class of Hamiltonians (including many local stabilizer codes) and provide six examples: the Harper equation, the Baxter parafermionic spin chain, the Rabi model, the Kitaev toric code, the Haah cubic code (which we generalize to qudits), and the Kitaev honeycomb model. We obtain continuous-variable generalizations of all models, some of which are novel. The Baxter model is mapped to a chain of coupled oscillators and the Rabi model to the optomechanical radiation pressure Hamiltonian. The procedures also yield rotor versions of all models, five of which are novel many-body extensions of the almost Mathieu equation. The toric and cubic codes are mapped to lattice models of rotors, with the toric code case related to $U(1)$ lattice gauge theory.

I. INTRODUCTION

Continuous-variable (CV) limits of discrete-variable (DV) systems, if done carefully, can yield new models which are both interesting and helpful in illuminating low-energy properties of the original DV systems. A physical example comes from spin-wave theory, where the Hamiltonian of interacting spins S is expanded in the limit of small quantum fluctuations ($S \gg 1$) using the Holstein-Primakoff mapping [1]. Another type of limit involves thinking of each DV system not as a spin, but as a finite quantum system [2] of dimension $\mathcal{N} = 2S + 1$ (in quantum information, a qu$\mathcal{N}$it) whose conjugate variables, position and momentum, are bounded and discrete. This DV → CV limit then involves making both variables continuous and unbounded. A less-used version makes one of the variables continuous and periodic (i.e., an angle) and the other an integer, resulting in the phase space of a rotor (DV → ROT; see Table I for all three phase spaces). While these limits deal with the underlying phase space of a DV system, it is not always clear when and how to apply them to specific DV Hamiltonians, particularly in composite scenarios (e.g., the Jaynes Cummings model) consisting of both DV and CV components. We attempt to address these issues by outlining general and straightforward limit-taking procedures and applying them to obtain known and new DV, ROT, and CV extensions of six well-known models from condensed-matter physics and quantum computation (see Table II).

In Sec. II, we provide a basic introduction of the three aforementioned phase spaces (DV, ROT, and CV) such that the latter two can be thought of as limits of the former. In turn, DV phase space can be understood as a discretization of CV phase space in terms of fixed position and momentum increments δx and δp (similar to a computer approximating differential equations with difference equations). Section III outlines all limit-taking procedures, with comments on when DV → CV can be a valid low-energy approximation of a DV Hamiltonian. We warm up with a known and exactly-solvable example of all limit-taking procedures — the harmonic oscillator AKA the Harper equation — in Sec. IV. In Sec. V, we study a many-body coupled-oscillator example — the Baxter $\mathbb{Z}_\mathcal{N}$ parafermionic spin chain. In Sec. VI, we introduce the Rabi model, show that its $\mathcal{N}$-state extension has a dihedral symmetry, and provide its analogues in all three phase spaces. We continue with deriving the CV toric code model from the DV one while introducing novel rotor toric code extensions in Sec. VII. In Sec. VIII, we develop DV, ROT, and CV extensions of the Haah cubic code. The Kitaev honeycomb model is generalized in Sec. IX. A final discussion is given in Sec. X.

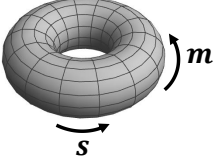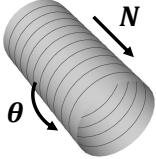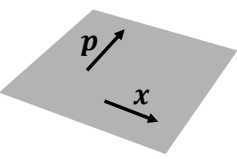* valbert4@gmail.com
† michel.devoret@yale.edu

	DV	ROT	CV
Sketch	m s	N θ	p x
Phase space	$(s,m) \in \mathbb{Z}_{\mathcal{N}} \times \mathbb{Z}_{\mathcal{N}}$	$(e^{i\theta}, N) \in \mathbb{T} \times \mathbb{Z}$	$(x,p) \in \mathbb{R} \times \mathbb{R}$
Weyl relation	$e^{-i\frac{2\pi}{\mathcal{N}}\boldsymbol{m}} e^{i\frac{2\pi}{\mathcal{N}}\boldsymbol{s}} e^{i\frac{2\pi}{\mathcal{N}}\boldsymbol{m}} e^{-i\frac{2\pi}{\mathcal{N}}\boldsymbol{s}} = e^{-i\frac{2\pi}{\mathcal{N}}}$	$e^{-i\boldsymbol{N}} e^{i\boldsymbol{\theta}} e^{i\boldsymbol{N}} e^{-i\boldsymbol{\theta}} = e^{-i}$	$e^{-i\boldsymbol{p}} e^{i\boldsymbol{x}} e^{i\boldsymbol{p}} e^{-i\boldsymbol{x}} = e^{-i\hbar}$
CCR	" $[\boldsymbol{s},\boldsymbol{m}] = i\dfrac{\mathcal{N}}{2\pi}$ "	" $[\boldsymbol{\theta},\boldsymbol{N}] = i$ "	$[\boldsymbol{x},\boldsymbol{p}] = i\hbar$
Fourier	Discrete Fourier transform	Fourier series	Fourier transform
"Bases"	$G(\boldsymbol{s})\lvert s\rangle = G(s)\lvert s\rangle$ $G(\boldsymbol{m})\lvert m\rangle = G(m)\lvert m\rangle$	$K(\boldsymbol{\theta})\lvert\theta\rangle = K(\theta)\lvert\theta\rangle$ $\boldsymbol{N}\lvert N\rangle = N\lvert N\rangle$	$\boldsymbol{x}\lvert x\rangle = x\lvert x\rangle$ $\boldsymbol{p}\lvert p\rangle = p\lvert p\rangle$
Translations	$e^{-i\frac{2\pi}{\mathcal{N}}\mathcal{M}\boldsymbol{m}}\lvert s\rangle = \lvert s+\mathcal{M}\rangle$ $e^{i\frac{2\pi}{\mathcal{N}}\mathcal{M}\boldsymbol{s}}\lvert m\rangle = \lvert m+\mathcal{M}\rangle$	$e^{-i\vartheta\boldsymbol{N}}\lvert\theta\rangle = \lvert\theta+\vartheta\rangle$ $e^{i\mathcal{M}\boldsymbol{\theta}}\lvert N\rangle = \lvert N+\mathcal{M}\rangle$	$e^{-i\xi\boldsymbol{p}}\lvert x\rangle = \lvert x+\xi\rangle$ $e^{i\xi\boldsymbol{x}}\lvert p\rangle = \lvert p+\xi\rangle$
Character	$\langle s\lvert m\rangle = \frac{1}{\sqrt{\mathcal{N}}} e^{i\frac{2\pi}{\mathcal{N}}sm}$	$\langle\theta\lvert N\rangle = \frac{1}{\sqrt{2\pi}} e^{i\theta N}$	$\langle x\lvert p\rangle = \frac{1}{\sqrt{2\pi}} e^{ixp}$
Relationship between bases	$\lvert m\rangle = \frac{1}{\sqrt{\mathcal{N}}} \sum\limits_{s\in\mathbb{Z}_{\mathcal{N}}} e^{i\frac{2\pi}{\mathcal{N}}sm}\lvert s\rangle$ $\lvert s\rangle = \frac{1}{\sqrt{\mathcal{N}}} \sum\limits_{m\in\mathbb{Z}_{\mathcal{N}}} e^{-i\frac{2\pi}{\mathcal{N}}sm}\lvert m\rangle$	$\lvert N\rangle = \frac{1}{\sqrt{2\pi}} \int_{-\pi}^{\pi} d\theta\, e^{i\theta N}\lvert\theta\rangle$ $\lvert\theta\rangle = \frac{1}{\sqrt{2\pi}} \sum\limits_{N\in\mathbb{Z}} e^{-i\theta N}\lvert N\rangle$	$\lvert p\rangle = \frac{1}{\sqrt{2\pi}} \int_{-\infty}^{\infty} dx\, e^{ixp}\lvert x\rangle$ $\lvert x\rangle = \frac{1}{\sqrt{2\pi}} \int_{-\infty}^{\infty} dp\, e^{-ixp}\lvert p\rangle$
Completeness	$\sum\limits_{s\in\mathbb{Z}_{\mathcal{N}}}\lvert s\rangle\langle s\rvert = \sum\limits_{m\in\mathbb{Z}_{\mathcal{N}}}\lvert m\rangle\langle m\rvert = \mathbf{1}$	$\sum\limits_{N\in\mathbb{Z}}\lvert N\rangle\langle N\rvert = \int_{-\pi}^{\pi}\frac{d\theta}{2\pi}\lvert\theta\rangle\langle\theta\rvert = \mathbf{1}$	$\int_{-\infty}^{\infty} dx\lvert x\rangle\langle x\rvert = \int_{-\infty}^{\infty} dp\lvert p\rangle\langle p\rvert = \mathbf{1}$
Orthonormality	$\sum\limits_{s\in\mathbb{Z}_{\mathcal{N}}} \frac{e^{i\frac{2\pi}{\mathcal{N}}(m-m')s}}{\mathcal{N}} = \delta_{m,m'}$ $\sum\limits_{m\in\mathbb{Z}_{\mathcal{N}}} \frac{e^{i\frac{2\pi}{\mathcal{N}}(s-s')m}}{\mathcal{N}} = \delta_{s,s'}$	$\int_{-\pi}^{\pi}\frac{d\theta}{2\pi} e^{i(N-N')\theta} = \delta_{N,N'}$ $\sum\limits_{N\in\mathbb{Z}} \frac{e^{i(\theta-\theta')N}}{2\pi} = \delta(\theta-\theta')$	$\int_{-\infty}^{\infty}\frac{dx}{2\pi} e^{i(p-p')x} = \delta(p-p')$ $\int_{-\infty}^{\infty}\frac{dp}{2\pi} e^{i(x-x')p} = \delta(x-x')$

Table I. Comparison and summary of relations between conjugate variables in DV-, ROT-, and CV-type phase spaces. Most physically relevant phase spaces consist of combinations of these three. An extension of the present analysis can be performed for any (locally compact) Abelian group [3] and for (compact) non-Abelian groups [4] (if one is willing to allow commutators to be non-trivial operators, thereby dropping the notion of a phase space). The (Abelian) groups involved here are $\mathbb{Z}_{\mathcal{N}} = \{-\lfloor\mathcal{N}/2\rfloor, \cdots, \lfloor(\mathcal{N}-1)/2\rfloor\}$, the circle group $\mathbb{T} = \{e^{i\theta}\,\lvert\,\theta \in [-\pi,\pi[\}$, the integers $\mathbb{Z}$, and the reals $\mathbb{R}$. The variables $\mathcal{M} \in \mathbb{Z}$, $\vartheta \in [-\pi,\pi[$, and $\xi \in \mathbb{R}$. In order to respect the domains of their respective conjugate variables, the functionals G and K are respectively $\mathcal{N}$- and 2π-periodic in their arguments. The canonical commutation relations (CCR's) in quotes are incorrect due to not preserving domains, but nevertheless give the right physical intuition. The label "Bases" is in quotes because $\lvert\theta\rangle$, $\lvert x\rangle$, and $\lvert p\rangle$ are not normalizable. See related tables in Refs. [3, 5].

II. CLASSICAL AND QUANTUM PHASE SPACES

A. Classical phase space

In classical physics, the phase space of a physical system with one degree of freedom is a two-dimensional manifold spanned by two infinitesimal translation generators, T_{dx} and T_{dp}, acting on the conjugate variables position and momentum, respectively. These translation operators commute,

$$T_{dx}T_{dp}T_{dx}^{-1}T_{dp}^{-1} = \mathrm{Id}. \tag{1}$$

Starting with the system located at an origin point, it is possible to reach a unique state in which the system is located at a well-defined phase space point (x,p) using a sequence of elementary translations. The infinitesimal circuit associated with the sequence of translations from Eq. (1) defines a surface element of phase space (see Fig. 1). Any observable over phase space $f(x,p)$ evolves in time according to Hamilton's equation, written here as

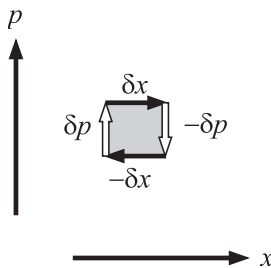$$df = \{H, f\}\, dt, \tag{2}$$

Figure 1. In phase space, four elementary translations along position and momentum define a closed circuit, here oriented clockwise, and its corresponding enclosed area, represented here in grey. Quantum physics associates a phase factor to an area in phase space, measured in units of Planck's constant.

where the Poisson bracket of two functions $A(x,p)$ and $B(x,p)$ of phase space is given by the exterior product

$$\{A,B\} = \frac{\partial A}{\partial x}\frac{\partial B}{\partial p} - \frac{\partial A}{\partial p}\frac{\partial B}{\partial x} \tag{3}$$

and $H(x,p)$ is the Hamiltonian function characterizing the dynamics of system. Note that the Hamiltonian does not set the nature of the degree of freedom itself, which is set by the topology of phase space. For instance, the phase space of a 1-D massive particle evolving in an x^2 potential (ideal harmonic oscillator) is a flat plane whereas the phase space of a rigid pendulum or a rotor is an infinite cylinder. While various phase spaces are used in classical mechanics (depending on constraints one puts on a particle's motion), there are only a few canonical topologies in quantum mechanics that meaningfully extend the classical notion of conjugate variables.

In order to be sufficiently general in our quantum mechanical treatment, instead of considering from the beginning a continuous phase space with infinitesimal generators T_{dx} and T_{dp}, we are going to introduce *finite* translation operators $T_{\delta x}$ and $T_{\delta p}$ and consider a topology of phase space where

$$(T_{\delta x})^{\mathcal{N}} = (T_{\delta p})^{\mathcal{N}} = \mathrm{Id}\,, \tag{4}$$

where $\mathcal{N}$ is a positive integer. Eventually, we will take the limits $\delta x \to 0$, $\delta p \to 0$ and $\mathcal{N} \to \infty$ in varying ways. We thus consider that our 1-D degree of freedom, instead of evolving continuously, hops from site to site, the set of sites forming a ring graph shown in Fig. 2(a). The position variable s denotes the site index and is thus an integer modulo $\mathcal{N}$, the total number of sites along the ring. If hopping between two sites takes the same universal amount of time, phase space is fully discrete, and the momentum m also belongs to the set of integers modulo $\mathcal{N}$. Because of periodic boundary conditions for both position and momentum, as indicated by the set of black and white arrows in Fig. 2(b), phase space has the topology of a torus.

B. Quantum phase space

In quantum physics, two conjugate translation generators do not commute, and one can categorize all possible relations into three cases:

$$T_{\delta x}T_{\delta p}T_{\delta x}^{-1}T_{\delta p}^{-1} \to C_{\delta x,\delta p} := e^{-i\frac{\delta x \boldsymbol{p}}{\hbar}} e^{i\frac{\delta p \boldsymbol{x}}{\hbar}} e^{i\frac{\delta x \boldsymbol{p}}{\hbar}} e^{-i\frac{\delta p \boldsymbol{x}}{\hbar}} = \begin{cases} 1 \\ e^{-i\frac{\delta x \delta p}{\hbar}} \\ \text{operator not-commuting with translations} \end{cases}. \tag{5}$$

The first case is obviously classical phase space. The second corresponds to a *quantum phase space* associated with a pair of Abelian groups of conjugate translations, typical of oscillators and rotors. The third case corresponds to spaces associated with non-Abelian groups, such as the $SU(2)$ group associated with a spin S (we discuss later how the $S = 1/2$ representation does produce the second case for particular $\delta x, \delta p$). In the following, we focus on the second case, that of a circuit in phase space producing a phase factor proportional to the area enclosed by the circuit, considering different limits for the step sizes δx and δp and the period $\mathcal{N}$. While we adhere to the definition of *quantum phase space* which corresponds only to the second case [3], we note that some of the properties we mention can also be extended to the third case [4].

Let us explore in detail the second case. Using Eqs. (4-5) to simplify $T_{\delta x}^{\mathcal{N}}T_{\delta p}^{\mathcal{N}}T_{\delta x}^{-\mathcal{N}}T_{\delta p}^{-\mathcal{N}}$, we can see that

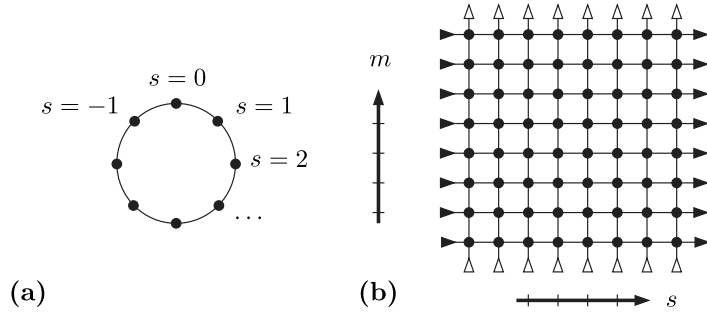$$(C_{\delta x,\delta p})^{\mathcal{N}} = \mathrm{Id}\,. \tag{6}$$

Figure 2. **(a)** The DV phase space can be thought of as consisting of a degree of freedom hopping from site to site. The set of sites forms a ring. The position variable s is a site index and is thus an integer modulo $\mathcal{N}$, the number of sites along the ring. **(b)** If hopping between two sites takes the universal same amount of time, phase space is fully discrete, with the momentum m belonging also to the set of integers modulo $\mathcal{N}$. Both position and momentum have periodic boundary conditions, as indicated by the set of black and white arrows, and thus phase space has the topology of a torus.

Since $C_{\delta x, \delta p}$ commutes with every operator in the algebra associated with the translations, we can represent it as

$$C_{\delta x, \delta p} \to e^{-i\frac{2\pi}{\mathcal{N}}} . \tag{7}$$

In our limit-taking procedures, the parameters δx, δp and $\mathcal{N}$ do not vary independently, and we impose

$$\frac{2\pi}{\mathcal{N}} = \frac{\delta x \delta p}{\hbar} . \tag{8}$$

In other words, $C_{\delta x, \delta p} \to e^{-i\frac{\delta x \delta p}{\hbar}}$, which corresponds to an elementary circuit in phase space accumulating a phase shift given by the encircled area divided by Planck's constant, in similarity with Bohr's old trajectory quantification rule.

Representing finite translations by exponentiation of translation generators (which we denote in bold),

$$T_{\delta x} \to e^{+i\frac{\delta x \boldsymbol{p}}{\hbar}} \tag{9a}$$

$$T_{\delta p} \to e^{-i\frac{\delta p \boldsymbol{x}}{\hbar}} , \tag{9b}$$

we can rewrite the *Weyl relation* as

$$e^{i\frac{\delta p \boldsymbol{x}}{\hbar}} e^{i\frac{\delta x \boldsymbol{p}}{\hbar}} e^{-i\frac{\delta p \boldsymbol{x}}{\hbar}} = e^{i\frac{\delta x}{\hbar}(\boldsymbol{p}-\delta p)} = e^{-i\frac{\delta x \delta p}{\hbar}} e^{i\frac{\delta x \boldsymbol{p}}{\hbar}} . \tag{10}$$

By naive expansion, we can recover the well-known result that the Weyl relation for the $T's$ is equivalent to the *canonical commutation relation* (CCR) for the corresponding generating operators

$$[\boldsymbol{x}, \boldsymbol{p}] = i\hbar . \tag{11}$$

The generators $\boldsymbol{x}$ and $\boldsymbol{p}$ and the commutation relation above define the algebra $\mathfrak{h}_4$ [6] (sometimes referred to as the Heisenberg-Weyl algebra [7]), which has only infinite-dimensional representations. We will review how the generators of motion for all common quantum-mechanical phase spaces, some of which are finite-dimensional, nevertheless emulate $\mathfrak{h}_4$ (see Table I, fourth row).

C. Toroidal doubly-discrete quantum phase space (DV)

In the algebra representing the translation operators, the relations (5) and (7) have important consequences. Let us introduce the projectors Π_s and Π_m over respective regions of phase space $s \cdot \delta x$ and $m \cdot \delta p$, where δx and δp are some small intervals which can be thought of as discretizations of ordinary continuous phase space and

$$s, m \in \{-\lfloor \mathcal{N}/2 \rfloor, \cdots, \lfloor (\mathcal{N}-1)/2 \rfloor\} =: \mathbb{Z}_{\mathcal{N}} . \tag{12}$$

We later vary the intervals δx and δp in a way which converts the DV phase space (and its associated Hilbert space) into the ROT and CV phase spaces. We have made the ranges of s, m "two-sided", i.e., defined them such that

both their maximum and minimum values are functions of $\mathcal{N}$, in order to properly perform said procedures. The projectors (by definition, $\Pi_s = \Pi_s^2$ and $\Pi_m = \Pi_m^2$) satisfy

$$T_{\delta x} \Pi_s T_{\delta x}^{-1} = \Pi_{s+1 \bmod \mathcal{N}} \tag{13a}$$

$$T_{\delta p} \Pi_s T_{\delta p}^{-1} = \Pi_s \tag{13b}$$

$$T_{\delta p} \Pi_m T_{\delta p}^{-1} = \Pi_{m+1 \bmod \mathcal{N}} \tag{13c}$$

$$T_{\delta x} \Pi_m T_{\delta x}^{-1} = \Pi_m \,. \tag{13d}$$

Quantum-mechanically, due to the non-commutation of conjugate translation operators, the product of projectors on position and momentum $\Pi_s \Pi_m$ can no longer be a projector (as in the classical case). Thus, $(\Pi_s \Pi_m)^2 \neq \Pi_s \Pi_m$ since the projectors do not commute and it is not possible to identify a phase space point state with both definite position s and momentum m. As a consequence of projections on m conflicting with projections on s, we have the discrete Fourier relations

$$|m\rangle = \frac{1}{\sqrt{\mathcal{N}}} \sum_{s \in \mathbb{Z}_\mathcal{N}} e^{i \frac{2\pi s m}{\mathcal{N}}} |s\rangle \qquad \text{and} \qquad |s\rangle = \frac{1}{\sqrt{\mathcal{N}}} \sum_{m \in \mathbb{Z}_\mathcal{N}} e^{-i \frac{2\pi m s}{\mathcal{N}}} |m\rangle \,, \tag{14}$$

where the position state vectors $|s\rangle$ and momentum state vectors $|m\rangle$ are defined as the eigenvectors of the projectors with eigenvalues 0 and 1:

$$\Pi_s |s'\rangle = \delta_{s',s} |s'\rangle \qquad \text{and} \qquad \Pi_m |m'\rangle = \delta_{m',m} |m'\rangle \,. \tag{15}$$

The projectors in the position basis and in the momentum basis both resolve the identity,

$$\sum_{s \in \mathbb{Z}_\mathcal{N}} |s\rangle \langle s| = \sum_{s \in \mathbb{Z}_\mathcal{N}} \Pi_s = \mathbf{1} \qquad \text{and} \qquad \sum_{m \in \mathbb{Z}_\mathcal{N}} |m\rangle \langle m| = \sum_{m \in \mathbb{Z}_\mathcal{N}} \Pi_m = \mathbf{1} \,, \tag{16}$$

and the overlap amplitude of the basis vectors is a constant,[1]

$$\langle s|m\rangle = \frac{1}{\sqrt{\mathcal{N}}} e^{i \frac{2\pi s m}{\mathcal{N}}} \qquad \text{implies} \qquad |\langle s|m\rangle|^2 = \frac{1}{\mathcal{N}} \,. \tag{17}$$

There are thus only $\mathcal{N} - 1$ independent projectors whereas there are $\mathcal{N}^2$ orthogonal observables (counting the identity as the constant observable). Classically, there would be also $\mathcal{N}^2$ orthogonal observables, but there would be also as much as $\mathcal{N}^2 - 1$ projectors. Thus, in quantum mechanics, the number of independent pure states is much less than the number of properties that can be acquired from them!

   Let us now introduce the conjugate variables that label states of fixed position and momentum,

$$\boldsymbol{s} = \sum_{s \in \mathbb{Z}_\mathcal{N}} s |s\rangle \langle s| \qquad \text{and} \qquad \boldsymbol{m} = \sum_{m \in \mathbb{Z}_\mathcal{N}} m |m\rangle \langle m| \,, \tag{18}$$

and quantify their conjugate nature. These operators label the columns and the rows of Fig. 2b, but again the non-commutation of these operators prevents simultaneously assigning a fixed position and momentum to the points in the corresponding classical space. The quantum or discrete Fourier transform operator going from the momentum basis to the position basis is

$$\boldsymbol{F}_{\text{DV}} \coloneqq \sum_{s \in \mathbb{Z}_\mathcal{N}} |s\rangle \langle m = s| = \frac{1}{\sqrt{\mathcal{N}}} \sum_{s \in \mathbb{Z}_\mathcal{N}} \sum_{s' \in \mathbb{Z}_\mathcal{N}} e^{i \frac{2\pi s s'}{\mathcal{N}}} |s\rangle \langle s'| \,. \tag{19}$$

The position and momentum operators are related by this transform via

$$\boldsymbol{F}_{\text{DV}}^\dagger \boldsymbol{m} \boldsymbol{F}_{\text{DV}} = \boldsymbol{s} \qquad \text{and} \qquad \boldsymbol{F}_{\text{DV}}^\dagger \boldsymbol{s} \boldsymbol{F}_{\text{DV}} = -\boldsymbol{m} \,. \tag{20}$$

Performing the discrete Fourier transform twice yields the DV parity operator

$$\boldsymbol{F}_{\text{DV}}^2 = \sum_{s \in \mathbb{Z}_\mathcal{N}} |-s\rangle \langle s| \,. \tag{21}$$

---

[1] A pair of bases for which the norm of the overlap between their constituents is independent of the basis labels is called *mutually unbiased* [8].

This important operator takes $\boldsymbol{s}, \boldsymbol{m}$ to $-\boldsymbol{s}, -\boldsymbol{m}$ modulo $\mathcal{N}$.

We can readily make contact with standard Fourier analysis by linking a quantum pure state $|\psi\rangle$ to a function of a discrete periodic variable ψ_m. Namely, writing $|\psi\rangle$ using the position basis and looking at the overlap of $|\psi\rangle$ with a momentum eigenstate $|m\rangle$ produces the discrete Fourier series of ψ_m:

$$|\psi\rangle = \sum_{s\in\mathbb{Z}_\mathcal{N}} \psi_s|s\rangle \quad \Leftrightarrow \quad \psi_m \coloneqq \langle m|\psi\rangle = \frac{1}{\sqrt{\mathcal{N}}} \sum_{s\in\mathbb{Z}_\mathcal{N}} \psi_s e^{-i\frac{2\pi sm}{\mathcal{N}}} . \tag{22}$$

The same holds for the dual momentum basis.

In the position state vector basis, translations in position and in momentum are explicitly given by[2]

$$T_{\delta x} \to \boldsymbol{X} \coloneqq e^{-i\frac{2\pi}{\mathcal{N}}\boldsymbol{m}} = \sum_{s\in\mathbb{Z}_\mathcal{N}} |s+1\mathrm{mod}\mathcal{N}\rangle\langle s| \tag{23a}$$

$$T_{\delta p} \to \boldsymbol{Z} \coloneqq e^{+i\frac{2\pi}{\mathcal{N}}\boldsymbol{s}} = \sum_{s\in\mathbb{Z}_\mathcal{N}} e^{+i\frac{2\pi s}{\mathcal{N}}} |s\rangle\langle s| , \tag{23b}$$

and such operators naturally perform displacements along the ring of sites in either position or momentum cross-sections of phase space:[3]

$$\boldsymbol{X}^\dagger \boldsymbol{s} \boldsymbol{X} = (\boldsymbol{s}+1)\,\mathrm{mod}\mathcal{N} \qquad \text{and} \qquad \boldsymbol{Z}^\dagger \boldsymbol{m} \boldsymbol{Z} = (\boldsymbol{m}+1)\,\mathrm{mod}\mathcal{N} . \tag{24}$$

Strictly speaking, we cannot relate the Weyl relation

$$\boldsymbol{X}\boldsymbol{Z}\boldsymbol{X}^\dagger\boldsymbol{Z}^\dagger = e^{-i\frac{2\pi}{\mathcal{N}}} \tag{25}$$

to a CCR since expanding $\boldsymbol{X}, \boldsymbol{Z}$ to first order will violate our imposed domains on $\boldsymbol{s}, \boldsymbol{m}$ [18]. In other words, $\boldsymbol{s}, \boldsymbol{m}$ can only be inside functions that are periodic in $\mathcal{N}$. However, we can depart from mathematical rigor and represent the above Weyl relation as the CCR

$$\text{``}\,[\boldsymbol{s}, \boldsymbol{m}] = i\frac{\mathcal{N}}{2\pi}\,\text{''} , \tag{26}$$

which is analogous to the continuous case (11). Moreover, if we express everything in terms of

$$\boldsymbol{x}_{\mathrm{DV}} \coloneqq \delta x\,\boldsymbol{s} \qquad \text{and} \qquad \boldsymbol{p}_{\mathrm{DV}} \coloneqq \delta p\,\boldsymbol{m} \tag{27}$$

and use our imposed phase space area constraint (8), the translations can be expressed as $\boldsymbol{X} = e^{-i\frac{\delta x}{\hbar}\boldsymbol{p}_{\mathrm{DV}}}$ and $\boldsymbol{Z} = e^{+i\frac{\delta p}{\hbar}\boldsymbol{x}_{\mathrm{DV}}}$ and Eq. (26) recovers the ordinary CCR "$[\boldsymbol{x}_{\mathrm{DV}}, \boldsymbol{p}_{\mathrm{DV}}] = i\hbar$" (11).

We briefly describe a Wigner function representation for DV for $\mathcal{N}$ being odd [2]. Recall that CV Wigner functions can be expressed in terms of the trace of a density matrix with a certain displaced parity operator; we provide the expression later in Eq. (40). In DV, an analogous expression is

$$W_{\mathrm{DV}}(S, M) = \frac{1}{\mathcal{N}} \sum_{s=0}^{\mathcal{N}-1} \langle s|\rho \boldsymbol{D}_{\mathrm{DV}}^{S,M} \boldsymbol{F}_{\mathrm{DV}}^2 \boldsymbol{D}_{\mathrm{DV}}^{S,M\dagger}|s\rangle = \frac{1}{\mathcal{N}} \mathrm{Tr}\left\{\rho \boldsymbol{D}_{\mathrm{DV}}^{S,M} \boldsymbol{F}_{\mathrm{DV}}^2 \boldsymbol{D}_{\mathrm{DV}}^{S,M\dagger}\right\} , \tag{28}$$

where $S, M \in \mathbb{Z}_\mathcal{N}$, ρ is an $\mathcal{N}\times\mathcal{N}$ density matrix, $\boldsymbol{F}_{\mathrm{DV}}^2$ (21) is the DV parity operator, and $\boldsymbol{D}_{\mathrm{DV}}^{S,M} \coloneqq e^{-i\frac{\pi SM}{\mathcal{N}}} e^{+i\frac{2\pi M}{\mathcal{N}}\boldsymbol{s}} e^{-i\frac{2\pi S}{\mathcal{N}}\boldsymbol{m}}$ is the DV displacement operator. The Wigner function conveniently takes real values over phase space and thus shares some of the properties of classical probability distributions, despite not always having positive values.

Properties of this DV fully discrete phase space for general $\mathcal{N}$ are summarized in the first column of Table I. We have only introduced the bare-bones framework, and there are many more quantities that can be defined in DV, including coherent states [19, 20], squeezed states [21], and quantum codes ([22]; [13], Sec. II). There are also plenty of other ways to visualize states [23–30]. We refer the reader to Refs. [2, 31–33] for further introductory reading.

―――――

[2] These were introduced first by Sylvester in the 19th century [9] and applied to quantum mechanics by von Neumann [10], Weyl [11], and Schwinger [12]. They have been called Schwinger bases, Weyl operators [3], Pauli operators [13], generalized spin [14] or Pauli [15] matrices, and 't Hooft generators or clock-and-shift matrices [16].

[3] The set $\{e^{i\frac{2\pi j}{\mathcal{N}}} e^{+i\frac{2\pi k}{\mathcal{N}}\boldsymbol{s}} e^{-i\frac{2\pi l}{\mathcal{N}}\boldsymbol{m}}\}_{j,k,l\in\mathbb{Z}_\mathcal{N}}$ forms a group, called the Generalized Pauli Group [15], and an algebra, sometimes called the non-commutative torus [17].

<center>*The $\mathcal{N} = 2$ case — a spin one-half system*</center>

It is important to realize that the case $\mathcal{N} = 2$ is that of the ubiquitous spin-$1/2$. In that case,

$$(T_{\delta x})^2 = \mathbf{1} \tag{29a}$$

$$(T_{\delta p})^2 = \mathbf{1} \tag{29b}$$

$$T_{\delta x} T_{\delta p} T_{\delta x}^{-1} T_{\delta p}^{-1} = T_{\delta x} T_{\delta p} T_{\delta x} T_{\delta p} = e^{-i\pi} \mathbf{1} = -\mathbf{1}. \tag{29c}$$

Therefore, $T_{\delta x} = \sigma_x$ and $T_{\delta p} = \sigma_z$. Since $\sigma_x = e^{i\frac{\pi}{2}(\sigma_x - \mathbf{1})}$ and same for σ_z, we have (modulo 2)

$$\boldsymbol{s} = \begin{pmatrix} -1 & 0 \\ 0 & 0 \end{pmatrix} = \frac{\sigma_z - \mathbf{1}}{2} \qquad \text{and} \qquad \boldsymbol{m} = \frac{\sigma_x - \mathbf{1}}{2}.$$

The Fourier transform corresponds to the well-known Hadamard transform and the parity operator (21) $\boldsymbol{F}_{\mathrm{DV}}^2 = \mathbf{1}$ is trivial. We thus see that at the particular angle $\theta = \pi/2$, the expression $e^{i\theta\sigma_x} e^{i\theta\sigma_z} e^{-i\theta\sigma_x} e^{-i\theta\sigma_z}$ does produce a constant not equal to one — the second case in Eq. (5). This does not occur for any other values of θ. Recalling that the generators $\{S_x, S_y, S_z\}$ of the $\mathfrak{su}(2)$ Lie algebra can be realized in a space of dimension $2S+1$ given a spin S [34], the $S = 1/2$ case at $\theta = \pi/2$ is the only time that spin rotations $\{e^{i\theta S_x}, e^{i\theta S_z}\}$ and DV translation operators $\{\boldsymbol{X}, \boldsymbol{Z}\}$ coincide. Therefore, procedures involving representations of $\mathfrak{su}(2)$ for $S > 1/2$, such as spin-coherent states [35], the Holstein-Primakoff transformation, and its associated Lie-algebraic contraction $(\mathfrak{u}(2) \to \mathfrak{h}_4$; see, e.g., [6, 36, 37]), are *not* directly connected to the phase space analysis discussed here for $\mathcal{N} > 2$.

D.   Cylindrical singly-discrete quantum phase space (ROT)

We now take the limit $\mathcal{N} \to \infty$, first considering the case where

$$\delta x = \frac{2\pi}{\mathcal{N}} \to 0 \qquad \text{and} \qquad \delta p = \mathcal{C}, \tag{30}$$

invoking a universal constant $\mathcal{C}$. Then we can introduce conjugate variables

$$\boldsymbol{\theta} \leftarrow \frac{2\pi}{\mathcal{N}} \boldsymbol{s} \qquad \text{and} \qquad \boldsymbol{N} \leftarrow \boldsymbol{m}. \tag{31}$$

The operators $\boldsymbol{\theta}$ and $\boldsymbol{N}$ take their eigenvalues in the set of angles (compact set of reals modulo 2π) and the set of all integers, respectively:

$$\theta \in [-\pi, \pi[\qquad \text{and} \qquad N \in \mathbb{Z}, \tag{32}$$

hence the renaming of $\boldsymbol{m}$ into $\boldsymbol{N}$.

In terms of wavefunctions, the limit as the number of points in the discretization $\mathcal{N} \to \infty$ is equivalent to the standard limit in which the discrete Fourier series of a *discrete* periodic wavefunction ψ_m is transformed into the ordinary Fourier series of a *continuous* periodic function (see [38], Sec. 3.4.5). In terms of the new conjugate variables, Eq. (22) becomes

$$\psi_m = \frac{1}{\sqrt{\mathcal{N}}} \sum_s \psi_s e^{-i\frac{2\pi sm}{\mathcal{N}}} = \frac{1}{\sqrt{2\pi}} \sum_\theta \psi(\theta) e^{-i\theta N} \frac{2\pi}{\mathcal{N}} \xrightarrow{\mathcal{N} \to \infty} \frac{1}{\sqrt{2\pi}} \int_{-\pi}^{\pi} \psi(\theta) e^{-i\theta N} d\theta, \tag{33}$$

where we have rescaled the coefficients as $\psi(\theta) \coloneqq \psi_m \sqrt{\mathcal{N}/2\pi}$. In the large $\mathcal{N}$ limit, this position-basis expansion of ψ becomes an integral over the angle θ. In this *infinite ladder* or ROT1 limit $(\boldsymbol{s}, \boldsymbol{m} \to \boldsymbol{\theta}, \boldsymbol{N})$, the circle labeled by eigenvalues of $\boldsymbol{m}$ is essentially "cut open" and turns into the unbounded integer-valued variable $\boldsymbol{N}$, while at the same time $\boldsymbol{s}$ is absorbed into the dense and bounded variable $\boldsymbol{\theta}$ conjugate to $\boldsymbol{N}$. Of course, one could have instead done $\boldsymbol{s}, \boldsymbol{m} \to \boldsymbol{N}, \boldsymbol{\theta}$, which we call the the *infinitely dense circle* or ROT2 limit. How the remaining properties of DV transform in this limit are listed in Table I. The concepts discussed for DV in the text, such as coherent states [39] and Wigner functions [40, 41], also naturally carry over to ROT (see also, e.g., [42, 43]).

In the ROT1 limit, DV position and momentum eigenstates (14) become

$$|\theta\rangle = \frac{1}{\sqrt{2\pi}} \sum_{N \in \mathbb{Z}} e^{-i\theta N} |N\rangle \qquad \text{and} \qquad |N\rangle = \frac{1}{\sqrt{2\pi}} \int_{-\pi}^{\pi} d\theta \, e^{i\theta N} |\theta\rangle, \tag{34}$$

respectively. Here, we encounter states which are normalizable only in the "Dirac" or "continuous" sense as well as the technicality that the orthonormality relation has to be 2π-periodic:

$$\langle \theta | \theta' \rangle = \frac{1}{2\pi} \sum_{N \in \mathbb{Z}} e^{-i(\theta'-\theta)N} = \sum_{N \in \mathbb{Z}} \delta\left(\theta' - \theta - 2\pi N\right) =: \delta^{(2\pi)}\left(\theta' - \theta\right). \tag{35}$$

Above, we define the 2π-periodic δ-function in order to make sure that we can use any values of θ [44]. However, if we restrict ourselves to using only $\theta \in [-\pi, \pi[$, as in Table I, the $\delta^{(2\pi)}$-function reduces to the ordinary δ-function. Since $|\theta\rangle$ are not normalizable, they technically do not belong to the function space $L^2(-\pi, \pi)$ associated with ROT, i.e., the space of functions $f(\theta)$ such that $\int d\theta |f(\theta)|^2 < \infty$ ([18], Sec. 6.6).

Another consequence of domains and similar to the DV case, the Weyl relation between translations in $\boldsymbol{N}$ and $\boldsymbol{\theta}$ does not imply a proper CCR (see Ref. [18], Sec. 12.2). Assuming that restrict ourselves to using only $\theta \in [-\pi, \pi[$, functions of $\boldsymbol{\theta}$ must be 2π-periodic in order to preserve its domain. Therefore, $\boldsymbol{\theta}$ and its powers cannot act on states alone. If we ignore this fact and calculate the variances of states $|n\rangle$ in $\boldsymbol{\theta}$ and $\boldsymbol{N}$, then we will see that the former yields a finite number while the latter is zero. This violates Heisenberg's uncertainty relation and thus the conventional CCR (we list what the CCR would have been if we did not worry about domains in Table I).

Application for the ROT phase space include i) the quantum rotor [44, 45], where N (θ) labels the angular momentum (position) of the rotor, ii) the motion of an electronic excitation in the periodic potential of crystal, where N is the site index, assuming the crystal to be infinite, which makes θ analogous to the pseudo momentum in band-theory [46], or iii) the dynamics of a Josephson junction between two isolated islands, like in the Cooper pair box [47, 48], where θ is the phase difference between the two superconductors on either side of the junction and N the number of Cooper pairs having tunneled across the junction.

E.   Flat-plane fully continuous quantum phase space (CV)

We again take the limit $\mathcal{N} \to \infty$, but now consider the case where both

$$\delta x = \delta p = \sqrt{\frac{2\pi}{\mathcal{N}}} \tag{36}$$

approach zero. Thus, while the whole of phase space has a number of points growing as $\mathcal{N}^2$, an area of order $\hbar$ will harbor of order $\mathcal{N}$ points and can still be considered continuous. Note that we did not have to split $2\pi/\mathcal{N}$ into two identical factors; any splitting $\delta x = (2\pi/\mathcal{N})^{1-\frac{\epsilon}{2}}$ and $\delta p = (2\pi/\mathcal{N})^{\frac{\epsilon}{2}}$ for $0 < \epsilon < 2$ is sufficient [49, 50]. Keeping with an even splitting, we introduce new conjugate variables

$$\boldsymbol{x} \leftarrow \sqrt{\frac{2\pi}{\mathcal{N}}} \, \boldsymbol{s} \qquad \text{and} \qquad \boldsymbol{p} \leftarrow \sqrt{\frac{2\pi}{\mathcal{N}}} \, \boldsymbol{m} \,, \tag{37}$$

which become ordinary position and momentum in the large $\mathcal{N}$ limit. We had already seen from Eq. (27) that this type of redefinition recovers the original commutation relation $[\boldsymbol{x}, \boldsymbol{p}] = i\hbar$ (11). In terms of wavefunctions, this is equivalent to the standard limit in which the discrete Fourier series of a periodic wavefunction ψ_m is transformed into the continuum Fourier series as the functions period $\mathcal{N} \to \infty$ (see [38], Sec. 3.4.5). In terms of the new conjugate variables, Eq. (22) becomes

$$\psi_m = \frac{1}{\sqrt{\mathcal{N}}} \sum_s \psi_s e^{-i\frac{2\pi sm}{\mathcal{N}}} = \frac{1}{\sqrt{2\pi}} \sum_p \psi(p) e^{-ixp} \delta p \xrightarrow{\mathcal{N} \to \infty} \frac{1}{\sqrt{2\pi}} \int_{-\infty}^{\infty} \psi(p) e^{-ixp} dp \,, \tag{38}$$

where $\psi(p) := \psi_s$. Since $\delta p \to 0$ for large $\mathcal{N}$, the above sum over p (38) becomes an integral over $\mathbb{R}$. This completes the limit-taking procedure $\boldsymbol{s}, \boldsymbol{m} \to \boldsymbol{x}, \boldsymbol{p}$. The properties of this continuous flat phase space are summarized in the last column of Table I. Just like $\boldsymbol{F}_{\text{DV}}$ (19), we can write the Fourier transform $\boldsymbol{F}_{\text{CV}}$ as a standalone operator:

$$\boldsymbol{F}_{\text{CV}} = \int_{-\infty}^{\infty} dx \, |x\rangle \langle p = x| = \frac{1}{\sqrt{2\pi}} \int_{-\infty}^{\infty} dx \int_{-\infty}^{\infty} dx' e^{ixx'} |x\rangle \langle x'| \,. \tag{39}$$

One can easily confirm that $\boldsymbol{F}_{\text{CV}}^2$ is the parity operator taking $\boldsymbol{x}, \boldsymbol{p} \to -\boldsymbol{x}, -\boldsymbol{p}$. Note that eigenfunctions $|x\rangle, |p\rangle$ of position and momentum are, like $|\theta\rangle$ (34), not normalizable and therefore not in the space of physical quantum states $L^2(\mathbb{R})$ ([18], Sec. 6.6).

	DV	ROT	CV
Sec. IV	Harper equation [55, 56]	Almost Mathieu equation [57]	Harmonic oscillator
Sec. V	Baxter $Z_\mathcal{N}$ parafermionic spin chain [58]	Rotor Baxter chain	Coupled-oscillator chain
Sec. VI	$\mathcal{N}$-state Rabi model [59–61]	Rotor-oscillator Rabi model	Optomechanical Hamiltonian
Sec. VII	Kitaev $\mathbb{Z}_\mathcal{N}$ toric code [62–64]	Rotor toric code	CV toric code [65]
Sec. VIII	Haah $\mathbb{Z}_\mathcal{N}$ cubic code [66]	Rotor Haah code	CV honeycomb model
Sec. IX	Kitaev honeycomb model [67–69]	Rotor honeycomb model	CV Haah code

Table II. The first column lists models to which we apply the limit-taking procedures of Sec. III, yielding the rotor (ROT) and continuous-variable (CV) models in the last two columns.

The CV Wigner function W_{CV} can then defined, analogous to W_{DV} (28), in terms of a CV displacement operator $\boldsymbol{D}_{\mathrm{CV}}^{X,P} \coloneqq e^{-iXP}e^{2iP\boldsymbol{x}}e^{-2iX\boldsymbol{p}}$ and the parity operator $\boldsymbol{F}_{\mathrm{CV}}^2$. One can easily confirm that $\boldsymbol{F}_{\mathrm{CV}}^2$ takes $\boldsymbol{x},\boldsymbol{p} \to -\boldsymbol{x},-\boldsymbol{p}$. Letting $X,P \in \mathbb{R}$ and following Appx. A.2.1 of Ref. [51] yields

$$W_{\mathrm{CV}}(X,P) = \frac{2}{\pi}\int_{-\infty}^{\infty} dx\langle x|\rho\boldsymbol{D}_{\mathrm{CV}}^{X,P}\boldsymbol{F}_{\mathrm{CV}}^2\boldsymbol{D}_{\mathrm{CV}}^{X,P\dagger}|x\rangle = \frac{2}{\pi}\mathrm{Tr}\left\{\rho\boldsymbol{D}_{\mathrm{CV}}^{X,P}\boldsymbol{F}_{\mathrm{CV}}^2\boldsymbol{D}_{\mathrm{CV}}^{X,P\dagger}\right\}. \tag{40}$$

Now that we have performed the DV $\to$ ROT and DV $\to$ CV limit-taking procedures, all that is left to complete the connections between them is the ROT $\to$ CV limit. Recall that the ROT variables are the angular $\boldsymbol{\theta}$ and integer $\boldsymbol{N}$. To perform the limit, we introduce a length scale $\mathcal{L}$ which rescales the periodicity of $\boldsymbol{\theta}$ and take this scale to infinity. The new variables this time are

$$\boldsymbol{x} \leftarrow \frac{\mathcal{L}}{2\pi}\boldsymbol{\theta} \qquad \text{and} \qquad \boldsymbol{p} \leftarrow \frac{2\pi}{\mathcal{L}}\boldsymbol{N}. \tag{41}$$

The first redefinition transforms the already continuous variable $\boldsymbol{\theta}$ into an unbounded variable while the second transforms the already unbounded variable $\boldsymbol{N}$ into a continuous one (since its intervals $\delta p \coloneqq \frac{2\pi}{\mathcal{L}}$ go to zero). In terms of the new conjugate variables, the $|\theta\rangle$ component of $|\psi\rangle$ expanded in the $|N\rangle$ basis becomes

$$\psi(\theta) \coloneqq \langle\theta|\psi\rangle = \frac{1}{\sqrt{2\pi}}\sum_{N\in\mathbb{Z}}\psi_N e^{i\theta N} = \frac{1}{\sqrt{2\pi}}\sum_p \psi(p)e^{-ixp}\delta p \xrightarrow{\mathcal{L}\to\infty} \frac{1}{\sqrt{2\pi}}\int_{-\infty}^{\infty}\psi(p)e^{-ixp}dp, \tag{42}$$

where we define the rescaled coefficients $\psi(p) \coloneqq \frac{\mathcal{L}}{2\pi}\psi_N$. This completes the last limit $\boldsymbol{\theta},\boldsymbol{N} \to \boldsymbol{x},\boldsymbol{p}$, which is based on the well-known conversion of a Fourier series of a periodic function $\psi(\theta)$ into a Fourier transform by taking the function's periodicity $\mathcal{L}$ to infinity.

Since the periodicity of both position and momentum goes to infinity, these DV $\to$ CV and ROT $\to$ CV limit-taking procedures are well adapted to studies of harmonic and weakly anharmonic oscillators and to expansions of periodic functions of operators. Letting x_{ZPF} and p_{ZPF} be standard deviations of the zero point fluctuations of the oscillator, we can introduce the operators $\boldsymbol{a}$ and $\boldsymbol{a}^\dagger$ such that

$$\boldsymbol{x} = x_{ZPF}\left(\boldsymbol{a}+\boldsymbol{a}^\dagger\right), \qquad \boldsymbol{p} = p_{ZPF}\left(\boldsymbol{a}-\boldsymbol{a}^\dagger\right)/i, \qquad \text{and} \qquad \left[\boldsymbol{a},\boldsymbol{a}^\dagger\right] = \boldsymbol{1}. \tag{43}$$

Then, the number of action quanta in the system is the operator

$$\boldsymbol{n} = \boldsymbol{a}^\dagger\boldsymbol{a}. \tag{44}$$

In general, the Hamiltonian is not a simple function of $\boldsymbol{n}$, but remains a balanced function of $\boldsymbol{a}$ and $\boldsymbol{a}^\dagger$. Using this notation, the Fourier transform and parity operator are simply

$$\boldsymbol{F}_{\mathrm{CV}} = e^{i\frac{\pi}{2}\boldsymbol{a}^\dagger\boldsymbol{a}} \qquad \text{and} \qquad \boldsymbol{F}_{\mathrm{CV}}^2 = (-1)^{\boldsymbol{a}^\dagger\boldsymbol{a}}. \tag{45}$$

Note that in contrast with the situation with the pair $\boldsymbol{N}$ and $\boldsymbol{\theta}$, there is no conjugate quantum operator for $\boldsymbol{n}$ satisfying all of the properties in Table I (although there is an operator satisfying some of the properties [52]). This is due to the fact that the polar representation of even a flat plane is singular when the radius is zero (equivalently, the eigenvalues of $\boldsymbol{n}$ are bounded from below). This effect also obstructs us from creating an orthonormal basis of phase states for quantum optical applications (see Ref. [53] or Ref. [54], Problem 8.4).

III. CONTINUUM AND ROTOR LIMIT-TAKING PROCEDURES

The above formulations of ROT and CV from DV are only done on the level of the Hilbert space. When it comes to applying them to Hamiltonians, there are some additional subtleties which have to be dealt with. In an attempt to resolve such subtleties, let us demonstrate our slightly generalized limit-taking procedures on a general DV-type Hamiltonian. Since we saw that there are two ways to take the DV → ROT limit in Sec. II D, the limits we consider below are summarized in the following diagram:

$$
\begin{array}{ccc}
 & \text{ROT1} & \\
 \nearrow & & \searrow \\
\text{DV} & \rightarrow & \text{CV} \\
 \searrow & & \nearrow \\
 & \text{ROT2} &
\end{array}
\tag{46}
$$

We start with a DV Hamiltonian that can be written as

$$
H_{\text{DV}} = -\frac{1}{2} \sum_k f_k \left(\frac{2\pi \mathcal{M}}{\mathcal{N}} \boldsymbol{s} \right) g_k \left(\frac{2\pi \mathcal{L}}{\mathcal{N}} \boldsymbol{m} \right) + H.c. ,
\tag{47}
$$

where $0 < \mathcal{M}, \mathcal{L} < \mathcal{N}$ modulate the hopping length scales for the respective variables and f_k, g_k are analytic $\mathcal{N}$-periodic functions of $\boldsymbol{s}, \boldsymbol{m}$ (18). Simpler versions of the DV → CV limit, which are applicable for all but one of the models we consider, can be performed with $\mathcal{M} = \mathcal{L} = 1$. However, these scales are necessary to be able to obtain CV via ROT, so we keep them for now.

Following Sec. II, we first write new conjugate variables in terms of $\boldsymbol{s}, \boldsymbol{m}$,

$$
\left(\frac{2\pi \mathcal{M}}{\mathcal{N}} \boldsymbol{s}, \frac{2\pi \mathcal{L}}{\mathcal{N}} \boldsymbol{m} \right) \rightarrow
\begin{cases}
\left(\sqrt{\dfrac{2\pi}{\mathcal{N}} \mathcal{L}} \boldsymbol{x}, \sqrt{\dfrac{2\pi}{\mathcal{N}} \mathcal{L}} \boldsymbol{p} \right) & \text{DV} \rightarrow \text{CV} \tag{48a} \\[2ex]
\left(\mathcal{M} \boldsymbol{\theta}, \dfrac{2\pi \mathcal{L}}{\mathcal{N}} \boldsymbol{N} \right) & \text{DV} \rightarrow \text{ROT1} \tag{48b} \\[2ex]
\left(\dfrac{2\pi \mathcal{M}}{\mathcal{N}} \boldsymbol{N}, \mathcal{L} \boldsymbol{\theta} \right) & \text{DV} \rightarrow \text{ROT2} \tag{48c}
\end{cases}
$$

where we have set $\mathcal{M} = \mathcal{L}$ for the first case because we do not need different length scales there. We then take the $\mathcal{N} \rightarrow \infty$ limit and write new Hamiltonians $H_{\text{CV}}, H_{\text{ROT1}}, H_{\text{ROT2}}$ which serve as extensions of H_{DV} into CV and ROT; the remainders of the respective limit-taking procedures are discussed in the next two subsections.

Previous efforts have rigorously studied similar embeddings in the past, in particular Barker [70–73] and Digernes et al. [74]. However, the former requires exact knowledge of the eigenstructure of both H_{DV} and $H_{\text{CV/ROT}}$ (see [72], Prop. 3.7) and is thus rigorously applicable to only simple examples. The latter constrains the Hamiltonian to be of a different form than H_{DV}. Here, we extend the procedure in the Supplement of Ref. [75] to any H_{DV} (in the language of [70], by "dead reckoning") with the goal of creating a meaningful extension of the DV system into CV and ROT. We apply these procedures to six models (see Table II), obtaining continuum and rotor generalizations that in some cases have not been known before. We sometime keep track of the symmetries of the model to demonstrate that our limits are symmetry-preserving.

A.   Continuum limit DV → CV

For this case, we take $\mathcal{N} \rightarrow \infty$ and expand around the center $(0,0)$ of $(\boldsymbol{s}, \boldsymbol{m})$-phase space. We could in principle expand around a generic point (s_0, m_0), but we can always redefine that to be the origin. This procedure can also be generalized to K DV systems $(\boldsymbol{s}, \boldsymbol{m})^{\otimes K}$; we stick to one for simplicity. First, let us take

$$
\frac{\mathcal{L}^2}{\mathcal{N}} \rightarrow 2\pi .
\tag{49}
$$

We perform this limit in order to remove any factors of $^1/\sqrt{\mathcal{N}}$ occurring in the expansion of some f_k, g_k later on, noting that it is not necessary if such factors occur for all k. The case when this step is necessary is only for the Rabi model in Sec. VI. We pick 2π in order to have the ROT → CV limits conveniently produce the same result as we are about to produce, but this is done for convention since a sequence of rational numbers can yield any real. As a sanity check, we see that that $\mathcal{L} = O(\sqrt{\mathcal{N}})$, i.e., the hopping between sites (determined by $\mathcal{L}$) does not increase faster than the total number of sites (proportional to $\mathcal{N}$).

Recalling that we have redefined variables as in Eq. (48a), let us approximate $f_k(2\pi\boldsymbol{x})$ and $g_k(2\pi\boldsymbol{p})$ with their expansions around the zero eigenvalue of $\boldsymbol{x}, \boldsymbol{p}$, respectively. Such an expansion can be done in a similar way as operator exponentiation, i.e., by working in a basis for which the two functions are diagonal and then expanding each of their eigenvalues. Such an expansion *will not* hold for arbitrarily high eigenvalues of H_{DV} since they are not always much less than one (e.g., near the maximal values of $\boldsymbol{s}, \boldsymbol{m}$). This means that, as $\mathcal{N} \to \infty$, we have to keep projecting ourselves to the intersection of the subspaces of small eigenvalues of $\boldsymbol{x}$ and $\boldsymbol{p}$. Consequently, the eigenstates of H_{DV} which remain in such a limit are only those which are centered around $(x, p) = (0, 0)$ and have small variance in either variable. Expanding, we obtain (apart from a constant shift in energy)

$$H_{\mathrm{DV}} \sim H_{\mathrm{CV}} \coloneqq -\sum_k A_k \boldsymbol{p} + B_k \boldsymbol{x} + \tfrac{1}{2} C_k \boldsymbol{p}^2 + \tfrac{1}{2} D_k \boldsymbol{x}^2 + E_k \boldsymbol{x}\boldsymbol{p} + E_k^\star \boldsymbol{p}\boldsymbol{x} \,, \tag{50}$$

with the coefficients A_k, B_k, C_k, D_k, E_k obvious functions of f_k, g_k and their derivatives (evaluated at zero). Thus, such a limit always yields a Hamiltonian consisting of linear and bilinear terms.

Let us discuss when the DV → CV limit corresponds to a physically meaningful low-energy expansion of H_{DV}. A trivial sufficient condition is that the ground state subspace of H_{DV} is localized around $(s, m) = (0, 0)$. That way, expansion around $(s, m) = (0, 0)$ encapsulates the ground state subspace and the low-energy excited states. If $f_k(0)g_k(0)$ is a global maximum for each k, then the minus sign in front of the sum (47) guarantees that the lowest-energy states will be centered around $(s, m) = (0, 0)$. [If there is another maximum at say $f_k(\mathcal{N}/2)g_k(\mathcal{N}/2)$ for all k, then expansion will of course ignore the ground state centered at $(\mathcal{N}/2, \mathcal{N}/2)$.] However, being centered at the origin still does not guarantee that the ground-state subspace is localized to the same degree in s as it is in m. Examples of systems whose ground states are centered but not equally localized around $(0, 0)$ are $H_{\mathrm{DV}} = -\cos(\frac{2\pi}{\mathcal{N}}\boldsymbol{s}) - \cos^{\lfloor J \rfloor}(\frac{2\pi}{\mathcal{N}}\boldsymbol{m})$ and $H_{\mathrm{DV}} = -\cos(\frac{2\pi}{\mathcal{N}}\boldsymbol{s}) - J\cos(\frac{2\pi}{\mathcal{N}}\boldsymbol{m})$ for $J \gg 1$. In both cases, the second term gives a higher energy penalty for states near the origin than the first term, so expanding only the second term is more appropriate. A similar example of such an expansion (albeit of ROT → CV type) is the expansion of the cosine term in the Josephson junction Hamiltonian,

$$\alpha \boldsymbol{N}^2 + \beta \cos \boldsymbol{\theta} \to \alpha \boldsymbol{p}^2 + \beta \boldsymbol{x}^2 \tag{51}$$

(where α, β are real and $\boldsymbol{N}, \boldsymbol{\theta}$ are ROT conjugate variables), to obtain the CV harmonic oscillator [47]. This limit is only valid in the $\beta \gg \alpha$ region of parameter space since only then the zero-point fluctuations in the phase are small — the ground state and its lowest-energy excitations are well-supported by the subspace of eigenstates $\{|\theta\rangle\}_{\theta \le \theta_{\max}}$ of $\boldsymbol{\theta}$ with $\theta_{\max} \ll 1$. We will not perform such limits here since they require certain terms to be more dominant than others; we assume that the contribution of all terms is approximately equal.

B. Rotor limits DV → ROT1, 2

These limits are considerably simpler than the continuum limit in that they only involve the hopping length scales $\mathcal{L}, \mathcal{M}$ and there is no expansion. For DV → ROT1 from Eq. (48b), we take $\mathcal{L}, \mathcal{N} \to \infty$ such that

$$\frac{\mathcal{L}}{\mathcal{N}} \to \Phi < 1 \,, \tag{52}$$

where Φ is irrational. The irrationality of Φ breaks the periodicity of g_k, yielding

$$H_{\mathrm{DV}} \sim H_{\mathrm{ROT1}} \coloneqq -\frac{1}{2} \sum_k f_k(\mathcal{M}\boldsymbol{\theta}) \, g_k(2\pi\Phi\boldsymbol{N}) + H.c. \,. \tag{53}$$

For the other limit DV → ROT2 in Eq. (48c), we let $\mathcal{M}/\mathcal{N} \to \Phi$, yielding

$$H_{\mathrm{DV}} \sim H_{\mathrm{ROT2}} \coloneqq -\frac{1}{2} \sum_k f_k(2\pi\Phi\boldsymbol{N}) \, g_k(\mathcal{L}\boldsymbol{\theta}) + H.c. \,. \tag{54}$$

These two limits are different whenever $f_k \ne g_k$ for some k.

There should not be any issues of physical validity with this limit (other than the fact that the system dimension is now infinite) since we are not expanding anything. Alternatively, we could expand g_k for all k, leaving f_k intact, given the assumption that low-energy states are more localized in $\boldsymbol{\theta}$ than in $\boldsymbol{N}$ (given $\mathcal{L} = 1$). As mentioned in the previous subsection, such a limit also yields interesting physics, but we do not delve too much on it here.

To complete the diagram (46), we can take the ROT1 → CV limit by letting $\mathcal{L} \to \infty$ and expanding f_k, g_k. Following Eq. (41), the new variables this time are $\boldsymbol{x} \leftarrow \frac{\mathcal{L}}{2\pi}\boldsymbol{\theta}$ and $\boldsymbol{p} \leftarrow \frac{2\pi}{\mathcal{L}}\boldsymbol{N}$. In addition, we take $\Phi \propto 1/\mathcal{L}$, where the proportionality constant can be any real number. We pick $\Phi = 2\pi/\mathcal{L}$ so that this expansion reproduces H_{CV} (50) within second order in $\boldsymbol{x}, \boldsymbol{p}$. The ROT2 → CV limit is performed the same manner, also yielding H_{CV}.
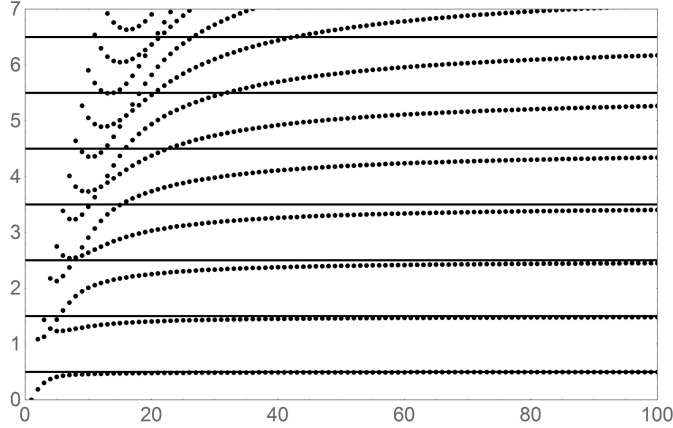
Figure 3. Eigenvalues of $\frac{\mathcal{N}}{2\pi}(H_{\mathrm{DV}}^{\mathrm{sho}} - 2)$ (56b) vs. $\mathcal{N}$ for $\mathcal{L} = \mathcal{M} = 1$. One can see that they approach true harmonic oscillator eigenvalues of an integer plus a half (horizontal lines) as $\mathcal{N} \to \infty$. This behavior persists for higher values of $\mathcal{L}$.

IV.   HARMONIC OSCILLATOR

Let us begin with the simple and known [55, 56, 75–77] example of DV and ROT analogues of the harmonic oscillator

$$H_{\mathrm{CV}}^{\mathrm{sho}} := \frac{1}{2}\left(\boldsymbol{p}^2 + \boldsymbol{x}^2\right). \tag{55}$$

First, consider a DV-type harmonic oscillator

$$H_{\mathrm{DV}}^{\mathrm{sho}} := -\frac{1}{2}\left(\boldsymbol{Z}^{\mathcal{M}} + H.c.\right) - \frac{1}{2}\left(\boldsymbol{X}^{\mathcal{L}} + H.c.\right) \tag{56a}$$

$$= -\cos\left(\frac{2\pi\mathcal{M}}{\mathcal{N}}\boldsymbol{s}\right) - \cos\left(\frac{2\pi\mathcal{L}}{\mathcal{N}}\boldsymbol{m}\right) \tag{56b}$$

$$= -\sum_{s\in\mathbb{Z}_{\mathcal{N}}}\cos\left(2\pi\frac{\mathcal{M}}{\mathcal{N}}s\right)|s\rangle\langle s| - \frac{1}{2}\sum_{s\in\mathbb{Z}_{\mathcal{N}}}\left(|s+\mathcal{L}\rangle\langle s| + |s\rangle\langle s+\mathcal{L}|\right), \tag{56c}$$

where we use $\boldsymbol{X}$ (23a) and $\boldsymbol{Z}$ (23b) in the first line and the basis $\{|s\rangle\}_{s\in\mathbb{Z}_{\mathcal{N}}}$ of eigenstates of $\boldsymbol{s}$ (18) in the last. This Hamiltonian corresponds to a quantum system on a ring with modulated periodic potential and an $\mathcal{L}$-site hopping term. We can certainly block diagonalize it into $\mathcal{L}$ blocks if $\mathcal{N}$ is a multiple of $\mathcal{L}$, but we do not concern ourselves with such special cases. This model is viewed as an analogue of the oscillator because one can recover $H_{\mathrm{CV}}^{\mathrm{sho}}$ in the DV → CV limit. We can already see the CV structure for $\mathcal{M} = 1$ if we recall that $\boldsymbol{Z} + \boldsymbol{Z}^\dagger$ is, up to a constant, the discrete Laplacian [74]; it will become an ordinary Laplacian in the limit below.

Applying the general technique of Sec. III A — setting $\mathcal{M} = \mathcal{L}$, redefining the conjugate variables (48a), expanding around $(s, m) = (0, 0)$ in the $\mathcal{N} \to \infty$ limit, and taking $\mathcal{L}^2/\mathcal{N} \to 2\pi$ — yields

$$H_{\mathrm{DV}}^{\mathrm{sho}} \sim \left(\mathcal{L}\sqrt{\frac{2\pi}{\mathcal{N}}}\right)^2 \cdot \frac{1}{2}\left(\boldsymbol{p}^2 + \boldsymbol{x}^2\right) = (2\pi)^2\, H_{\mathrm{CV}}^{\mathrm{sho}}. \tag{57}$$

To check this limit, we can plot the eigenvalues of $\frac{\mathcal{N}}{2\pi}(H_{\mathrm{DV}}^{\mathrm{sho}} - 2)$ for a given $\mathcal{L}$ and with increasing $\mathcal{N}$. As seen in Fig. 3, the eigenvalues approach those of the continuum harmonic oscillator. In fact, this limit has been proven to yield $H_{\mathrm{CV}}^{\mathrm{sho}}$ exactly (see example C.4 in Ref. [72] and references therein), so we are certain that the DV → CV limit is physically meaningful in this case. It should not be surprising since the ground state of $H_{\mathrm{DV}}^{\mathrm{sho}}$ is localized around $(s, m) = (0, 0)$ and expansion of both cosines adds the lowest possible energy penalty. Such a limit is also generalizable to $\mathcal{M} \neq \mathcal{L}$, allowing $H_{\mathrm{CV}}^{\mathrm{sho}}$ to have a free frequency parameter.

Now let us take $H_{\mathrm{DV}}^{\mathrm{sho}}$ to one of two ROT-type harmonic oscillators. Following Sec. III B, redefine variables as in Eq. (48b) and let $\mathcal{L}/\mathcal{N} \to \Phi$, yielding

$$H_{\mathrm{ROT1}}^{\mathrm{sho}} := -\cos(\mathcal{M}\boldsymbol{\theta}) - \cos(2\pi\Phi\boldsymbol{N}) \tag{58a}$$

$$= -\frac{1}{2}\sum_{N\in\mathbb{Z}}\left(|N+\mathcal{M}\rangle\langle N| + |N\rangle\langle N+\mathcal{M}|\right) - \sum_{N\in\mathbb{Z}}\cos(2\pi\Phi N)|N\rangle\langle N|, \tag{58b}$$

where $\Phi < 1$ is a positive irrational. In the context of the quantum Hall effect, $H_{\mathrm{ROT1}}^{\mathrm{sho}}$ models an electron on a 2D lattice in the presence of a magnetic field and Φ is the magnetic flux per unit cell. In that context, $H_{\mathrm{DV}}^{\mathrm{sho}}$ is called Harper's equation [78] and $H_{\mathrm{ROT1}}^{\mathrm{sho}}$ the almost Mathieu operator. In particular, $H_{\mathrm{ROT1}}^{\mathrm{sho}}$ with $\Phi = \frac{1}{2}(\sqrt{5}-1)$ corresponds to the Fibonacci quasicrystal [79]. There is of course another way to obtain an ROT-type Hamiltonian from $H_{\mathrm{DV}}^{\mathrm{sho}}$ by following Eq. (48c) and letting $\mathcal{M}/\mathcal{N} \to \Phi$, yielding the ROT2 Hamiltonian

$$H_{\mathrm{ROT2}}^{\mathrm{sho}} \coloneqq -\cos\left(2\pi\Phi\boldsymbol{N}\right) - \cos(\mathcal{L}\boldsymbol{\theta}) . \tag{59a}$$

In this case, the two ROT limits yield the same result.

Finishing off with the ROT $\to$ CV limit, let $\Phi \to {}^{2\pi}/\mathcal{L} \to 0$ and expand both cosine terms in $H_{\mathrm{ROT1}}^{\mathrm{sho}}, H_{\mathrm{ROT2}}^{\mathrm{sho}}$. In the aforementioned context of the quantum Hall effect, this limit is related to the quasiclassical limit of vanishing field and recovers the famous Landau-level problem [78] — a simple harmonic oscillator,

$$H_{\mathrm{ROT1}}^{\mathrm{sho}} \sim \frac{(\Phi\mathcal{L})^2}{2}\boldsymbol{p}^2 + \frac{(2\pi)^2}{2}\boldsymbol{x}^2 = (2\pi)^2\, H_{\mathrm{CV}}^{\mathrm{sho}} . \tag{60}$$

The result is thus the same as the direct DV $\to$ CV procedure from Eq. (57).

V. BAXTER $Z_\mathcal{N}$ PARAFERMIONIC SPIN CHAIN

Using Eqs. (23a-23b) for the Weyl operators $\boldsymbol{X}$ and $\boldsymbol{Z}$, the Baxter $\mathbb{Z}_\mathcal{N}$ spin chain Hamiltonian [58, 80, 81] (in Hermitian form) reads

$$H_{\mathrm{DV}}^{\mathrm{bax}} \coloneqq -\frac{\Omega}{2}\sum_{k=1}^{K}\left(\boldsymbol{Z}_k^\mathcal{M} + H.c.\right) - \frac{g}{2}\sum_{k=1}^{K-1}\left(\boldsymbol{X}_k^\mathcal{L}\boldsymbol{X}_{k+1}^{-\mathcal{L}} + H.c.\right) \tag{61a}$$

$$= -\Omega\sum_{k=1}^{K}\cos\left(\frac{2\pi\mathcal{M}}{\mathcal{N}}\boldsymbol{s}_k\right) - g\sum_{k=1}^{K-1}\cos\left(\frac{2\pi\mathcal{L}}{\mathcal{N}}\left[\boldsymbol{m}_{k+1} - \boldsymbol{m}_k\right]\right) , \tag{61b}$$

where the parameters Ω, g are of the same order of magnitude (so that we can expand both cosines). The $\mathcal{N} = 2$ case reduces to the original Ising model.[4] For general $\mathcal{N}$, each site k corresponds lives in its own DV phase space, and the full model is therefore in DV$^{\otimes K}$. One can also add phases (e.g., $\boldsymbol{Z}_k \to \boldsymbol{Z}_k e^{i\phi}$) [69], leading to more complicated behavior (similar to the chiral version of the Rabi model in Sec. VI). This model is equivalent to a parafermion chain via a nonlocal extension of the Jordan-Wigner transformation [85]. When written in terms of the conjugate variables $\{\boldsymbol{s},\boldsymbol{m}\}^{\otimes K}$, the model's (61b) invariance upon the collective translations $\boldsymbol{m}_k \to \boldsymbol{m}_k + 1$ and reflections $\boldsymbol{m}_k \to -\boldsymbol{m}_k$ (both for all k) are made bare. The operator for the former symmetry is simply $\boldsymbol{Z}^{\otimes K}$; we will keep track of this symmetry as the systems travels to the CV and ROT phase spaces.

We now apply the limit-taking procedures from Sec. III to $H_{\mathrm{DV}}^{\mathrm{sho}}$, obtaining its ROT and CV limits. If we take $H_{\mathrm{DV}}^{\mathrm{sho}}$ (56b) to be the canonical harmonic oscillator in DV phase space, then we can see that $H_{\mathrm{DV}}^{\mathrm{bax}}$ (61b) is nothing but a chain of coupled DV oscillators. It should thus not come as a surprise that the DV $\to$ CV limit, as we shall see, produces a chain of CV oscillators. Up to a constant offset and a multiplicative factor of $(2\pi)^2$, redefining variables per Eq. (48a) and expanding the cosines around $(s, m) = (0, 0)$ yields

$$H_{\mathrm{CV}}^{\mathrm{bax}} \coloneqq \frac{\Omega}{2}\sum_{k=1}^{K}\boldsymbol{p}_k^2 + \frac{g}{2}\sum_{k=1}^{K-1}\left(\boldsymbol{x}_{k+1} - \boldsymbol{x}_k\right)^2 . \tag{62}$$

The aforementioned symmetries clearly survive: $H_{\mathrm{CV}}^{\mathrm{bax}}$ is invariant under global reflection $\boldsymbol{x}_k \to -\boldsymbol{x}_k$ and any global shifts $\boldsymbol{x}_k \to \boldsymbol{x}_k + \xi$ for all k and any real ξ. It will interesting to see whether the spectrum of this simple model can be rigorously obtained in the large-$\mathcal{N}$ limit of the exact spectrum of the Baxter model, as was done for the oscillator [72].

Let us now turn the DV phase spaces of $H_{\mathrm{DV}}^{\mathrm{bax}}$ into infinite ladders (ROT1), taking the $\boldsymbol{s},\boldsymbol{m} \to \boldsymbol{N},\boldsymbol{\theta}$ limit from Sec. III B, yielding

$$H_{\mathrm{ROT1}}^{\mathrm{bax}} \coloneqq -\Omega\sum_{k=1}^{K}\cos\left(2\pi\Phi\boldsymbol{N}_k\right) - g\sum_{k=1}^{K-1}\cos\left(\mathcal{L}\left[\boldsymbol{\theta}_{k+1} - \boldsymbol{\theta}_k\right]\right) . \tag{63}$$

---

[4] Another generalization of the Ising model — the quantum Potts (e.g., [69, 82, 83]) or quantum clock [84] model — is not amenable to our limit-taking procedures because it contains a sum over all $\mathcal{L}, \mathcal{M}$ and so restricts us from having $\mathcal{L}, \mathcal{M} = O(\sqrt{\mathcal{N}})$ for large $\mathcal{N}$.

Expanding the first cosine in a limit $(\Omega \gg g)$ similar to that in eq. (51) immediately yields a Hamiltonian for an array of coupled Josephson Junctions in the quantum regime — the quantum XY model (e.g., [86, 87]). Alternatively, we can take the infinitely dense circle limit (ROT2), in which $\boldsymbol{s}, \boldsymbol{m} \to \boldsymbol{\theta}, \boldsymbol{N}$:

$$H_{\text{ROT2}}^{\text{bax}} \coloneqq -\Omega \sum_{k=1}^{K} \cos\left(\mathcal{M}\boldsymbol{\theta}_k\right) - g \sum_{k=1}^{K-1} \cos\left(2\pi\Phi\left[\boldsymbol{N}_{k+1} - \boldsymbol{N}_k\right]\right). \tag{64}$$

This corresponds to an infinite ladder of sites once more, but this time there is a hopping term and an interaction that is diagonal in the $\boldsymbol{N}$ basis. Expanding the latter in a procedure similar to that in eq. (51) yields a Hubbard model of sorts, with interactions of the form $(\boldsymbol{N}_{k+1} - \boldsymbol{N}_k)^2$. In both ROT versions, invariance under global reflection and shifts of all $\boldsymbol{\theta}_k$ $(\boldsymbol{N}_k)$ in the case ROT1 (ROT2) is preserved.

Both the ROT1 and ROT2 cases can then be taken to the CV case by performing the procedures described in Sec. IV for the simple harmonic oscillator. For $H_{\text{ROT1}}^{\text{bax}}$, take $\Phi = 2\pi/\mathcal{L}$, $\frac{\mathcal{L}}{2\pi}\boldsymbol{\theta} \to \boldsymbol{x}$, $\frac{2\pi}{\mathcal{L}}\boldsymbol{N} \to \boldsymbol{p}$, and $\mathcal{L} \to \infty$. For $H_{\text{ROT2}}^{\text{bax}}$, take $\Phi = 2\pi/\mathcal{M}$, $\frac{\mathcal{M}}{2\pi}\boldsymbol{\theta} \to \boldsymbol{p}$, $\frac{2\pi}{\mathcal{M}}\boldsymbol{N} \to \boldsymbol{x}$, and $\mathcal{M} \to \infty$. Both cases reduce those Hamiltonians to $H_{\text{CV}}^{\text{bax}}$ (62). These two limits are the reason we introduced both length scales $\mathcal{M}$ and $\mathcal{L}$ in $H_{\text{DV}}^{\text{bax}}$ (61a); performing the DV $\to$ CV procedure alone does not require them.

VI.   N-STATE RABI MODEL

The original quantum Rabi model Hamiltonian [59, 60] consists of an interacting two-level system (i.e., a qubit) and a harmonic oscillator and is arguably one of the simplest non-linear, non-trivial models. Letting σ_x, σ_z be the Pauli matrices of the qubit and $\mathbf{b}/\mathbf{b}^\dagger$ be the lowering/raising operators of the oscillator, the Rabi Hamiltonian is

$$\frac{1}{\hbar} H_{\mathcal{N}=2}^{\text{rabi}} \coloneqq \omega\left(\mathbf{b}^\dagger\mathbf{b} + \frac{1}{2}\right) - \Omega\sigma_z + g\left(\mathbf{b} + \mathbf{b}^\dagger\right)\sigma_x. \tag{65}$$

The three real parameters are the positive oscillator frequency ω, the qubit Larmor frequency Ω, and the qubit-oscillator coupling g. This model and its close relatives have been used in numerous contexts to simulate qubit-oscillator systems, including:

1. A two-level atom coupled to a cavity electromagnetic field in quantum optics and superconducting circuits. In this context, the model is a precursor to the Jaynes-Cummings model [88–90]: ignoring the term $\mathbf{b}\sigma_-$ and its conjugate (the rotating-wave approximation) yields that famous Hamiltonian.

2. A spinful electron coupled to a magnetic field; the related model is called the Landau level problem with Dresselhaus or Rashba spin-orbit coupling [91–93].

3. Ultra-cold alkali atoms in a magnetic field and double-well potential [94].

4. An exciton interacting with lattice vibrations at two sites of a crystalline system, where the model is called the single-mode spin boson or the two-site Holstein model [95, 96].

5. Strong magnetic coupling between an NV center and a nanomechanical oscillator in a longitudinal [97] or transverse [98] field.

Unlike the Jaynes-Cummings model, this model has a $\mathbb{Z}_2$ symmetry. Namely, the Hamiltonian commutes with

$$\boldsymbol{V}_{\mathcal{N}=2} = (-1)^{\mathbf{b}^\dagger\mathbf{b}}\sigma_z, \tag{66}$$

which squares to identity and represents a joint parity of the qubit and the oscillator [recall that $\boldsymbol{F}_{\text{CV}}^2 = (-1)^{\mathbf{b}^\dagger\mathbf{b}}$ (45)]. The model is also real, so $H_{\mathcal{N}=2}^{\text{rabi}}$ commutes with the complex conjugation operator K.

The $\mathcal{N}$-state Rabi model [61] is an extension of the qubit ($\mathcal{N} = 2$) Rabi model to qudits that naturally extends the symmetry of the qubit case:

$$\frac{1}{\hbar} H_{\text{DV}}^{\text{rabi}} \coloneqq \omega\left(\mathbf{b}^\dagger\mathbf{b} + \frac{1}{2}\right) - \frac{\Omega}{2}\left(\boldsymbol{Z}^{\mathcal{M}} + H.c.\right) + g\left(\mathbf{b}\boldsymbol{X}^{\mathcal{L}} + H.c.\right) \tag{67a}$$

$$= \omega\left(\mathbf{b}^\dagger\mathbf{b} + \frac{1}{2}\right) - \Omega\cos\left(\frac{2\pi\mathcal{M}}{\mathcal{N}}\boldsymbol{s}\right) + g\left(\mathbf{b}e^{-i\frac{2\pi\mathcal{L}}{\mathcal{N}}\boldsymbol{m}} + H.c.\right) \tag{67b}$$

(Note how the $\mathcal{N} = 2$ case reduces to the original Rabi model.) Originally, the $\mathcal{N}$-state Rabi model included more couplings using other powers of $\boldsymbol{Z}$, but we omit those for simplicity. The $\mathbb{Z}_2$ symmetry from the $\mathcal{N} = 2$ case generalizes to a $\mathbb{Z}_\mathcal{N}$ symmetry with generator

$$\boldsymbol{V} = e^{i\frac{2\pi}{\mathcal{N}}\mathcal{L}\,\mathbf{b}^\dagger\mathbf{b}}\boldsymbol{Z} = \exp\left[i\frac{2\pi}{\mathcal{N}}\left(\mathcal{L}\,\mathbf{b}^\dagger\mathbf{b} + \boldsymbol{s}\right)\right]. \tag{68}$$

We further say here that the model actually has a *dihedral* symmetry. In addition to $\boldsymbol{V}$, the Hamiltonian is invariant under the operation $\boldsymbol{s} \to -\boldsymbol{s}$. This reflection around the $\boldsymbol{m} = 0$ axis is represented by the antiunitary operator

$$\boldsymbol{U} \coloneqq \boldsymbol{F}_{\mathrm{DV}}^2 K\,, \tag{69}$$

where K is complex conjugation and $\boldsymbol{F}_{\mathrm{DV}}^2$ (21) is the DV parity operator taking $\boldsymbol{s}, \boldsymbol{m} \to -\boldsymbol{s}, -\boldsymbol{m}$ modulo $\mathcal{N}$. The full symmetry is then the dihedral group $D_{2\mathcal{N}} = \mathbb{Z}_\mathcal{N} \rtimes \mathbb{Z}_2$, where the $\mathbb{Z}_\mathcal{N}$ piece is generated by $\boldsymbol{V}$ while the $\mathbb{Z}_2$ piece is generated by $\boldsymbol{U}$. It is interesting to note that one can reduce the $\mathbb{Z}_\mathcal{N} \rtimes \mathbb{Z}_2$ symmetry to $\mathbb{Z}_\mathcal{N}$ by giving the cosine term a phase. In such a *chiral* version of the DV-type Rabi model [99], $\boldsymbol{s} \to -\boldsymbol{s}$ will no longer be a symmetry. Observing Eq. (67b), we can see that the qudit consists of a ring of $\mathcal{N}$ sites with energies $-\Omega\cos\left(2\pi\frac{\mathcal{M}}{\mathcal{N}}\boldsymbol{s}\right)$ and that the hopping term $\mathbf{b}e^{-i\frac{2\pi}{\mathcal{N}}\mathcal{L}\boldsymbol{m}}$ takes the qudit state $|s\rangle$ to the state $|s + \mathcal{L}\rangle$ while also absorbing a photon. The conjugate term corresponds to emitting a photon and moving $\mathcal{L}$ sites in the other direction along the qudit ring.

Let us perform the DV $\to$ CV limit from Sec. III A, which yields a CV phase space for the degrees of freedom of the $\mathcal{N}$-state system. Just like in for previous two models, we redefine variables according to Eq. (48a) and expand around the origin $(s, m) = (0, 0)$ of DV phase space. To our knowledge, the DV $\to$ CV limit is different from previous limits of the Rabi model, e.g., the large spin limit [100–102]. Letting $\boldsymbol{y} \coloneqq \frac{1}{\sqrt{2}}(\mathbf{b} + \mathbf{b}^\dagger)$ and $\boldsymbol{q} = -i\frac{1}{\sqrt{2}}(\mathbf{b} - \mathbf{b}^\dagger)$ (with $[\boldsymbol{y}, \boldsymbol{q}] = i$) be the original oscillator degrees of freedom (which remain unchanged), this yields

$$\frac{1}{\hbar}H_{\mathrm{CV}}^{\mathrm{rabi}} \coloneqq \frac{\omega}{2}\left(\boldsymbol{q}^2 + \boldsymbol{y}^2\right) + 2\Omega\pi^2\boldsymbol{p}^2 + \sqrt{2}g\left(2\pi\boldsymbol{x}\boldsymbol{q} + \boldsymbol{y}\left[1 - 2\pi^2\boldsymbol{x}^2\right]\right) - \Omega\,. \tag{70}$$

Displacing that oscillator by $-\frac{\sqrt{2}g}{\omega}$ [via the operator $\boldsymbol{D}$, which takes $\boldsymbol{y} \to \boldsymbol{y} - \frac{g}{\omega}$ and same with $\boldsymbol{q}$] gets rid of the linear $\boldsymbol{y}$ term and yields

$$\frac{1}{\hbar}\boldsymbol{D}H_{\mathrm{CV}}^{\mathrm{rabi}}\boldsymbol{D}^\dagger = \frac{\omega}{2}\left(\boldsymbol{q}^2 + \boldsymbol{y}^2\right) + 2\pi^2\left(\Omega\boldsymbol{p}^2 + \frac{2g^2}{\omega}\boldsymbol{x}^2\right) + 2\sqrt{2}g\pi\boldsymbol{x}\left(\boldsymbol{q} - \pi\boldsymbol{x}\boldsymbol{y}\right) - \left(\Omega + \frac{2g^2}{\omega}\right). \tag{71}$$

We thus see how the Rabi model reduces to a coupled oscillator model in the DV $\to$ CV limit. We can see that what is obtained is none other than the optomechanical Hamiltonian of a mechanical mode (which used to the $\mathcal{N}$-state system) interacting with a light mode via the $\boldsymbol{x}^2\mathbf{b}$ coupling. The $\sigma_+\mathbf{b}$ coupling induced by light on a two-level atom has become, in this limit, radiation pressure on an oscillator.

Performing the DV $\to$ ROT1, 2 limits from Sec. III B yields the respective coupled-rotor systems

$$\frac{1}{\hbar}H_{\mathrm{ROT1}}^{\mathrm{rabi}} \coloneqq \omega\left(\mathbf{b}^\dagger\mathbf{b} + \frac{1}{2}\right) - \Omega\cos\left(2\pi\Phi\boldsymbol{N}\right) + g\left(\mathbf{b}e^{-i\mathcal{L}\boldsymbol{\theta}} + H.c.\right) \tag{72}$$

$$\frac{1}{\hbar}H_{\mathrm{ROT2}}^{\mathrm{rabi}} \coloneqq \omega\left(\mathbf{b}^\dagger\mathbf{b} + \frac{1}{2}\right) - \Omega\cos\left(\mathcal{M}\boldsymbol{\theta}\right) + g\left(\mathbf{b}e^{-i2\pi\Phi\boldsymbol{N}} + H.c.\right). \tag{73}$$

The first model corresponds to an infinite ladder consisting of sites $|N\rangle$ in a Ω-mediated quasiperiodic potential and with the coupling term causing a particle on a site to move either to the left or right, depending on whether the particle absorbs or emits a photon. The second model corresponds to an infinite ladder of sites with hopping strength Ω, but this time each site $|N\rangle$ is linearly coupled to an oscillator with strength g and quasiperiodic phase $2\pi\Phi N$. Naturally, the dihedral ($D_{2\mathcal{N}} = \mathbb{Z}_\mathcal{N} \rtimes \mathbb{Z}_2$) symmetry of the DV-type Rabi model is extended to a $U(1) \rtimes \mathbb{Z}_2 = O(2)$ symmetry. The $U(1)$ piece is generated by $\mathcal{L}\mathbf{b}^\dagger\mathbf{b} + \boldsymbol{N}$ for ROT1 and by $2\pi\Phi\mathbf{b}^\dagger\mathbf{b} + \boldsymbol{\theta}$ for ROT2. The $\mathbb{Z}_2$ piece just corresponds to reflection: $\boldsymbol{N} \to -\boldsymbol{N}$ for ROT1 and $\boldsymbol{\theta} \to -\boldsymbol{\theta}$ for ROT2. Both $H_{\mathrm{ROT1}}^{\mathrm{rabi}}$ and $H_{\mathrm{ROT2}}^{\mathrm{rabi}}$ can then be taken to $H_{\mathrm{CV}}^{\mathrm{rabi}}$ (70) via the procedures described in Sec. III B.

VII. KITAEV TORIC CODE

The toric code [62] was proposed as a simple model for topological quantum computation. The degrees of freedom are qubits typically living on vertices of a square lattice with periodic boundary conditions (i.e., a torus). The Hamiltonian is written as a sum of products of four Weyl operators. We denote operators O acting nontrivially on

a site "•" on a plaquette "□" or vertex/star "+" as, e.g., $O_{\raisebox{-1pt}{\tiny■}}$ or $O_{\raisebox{-1pt}{\tiny+}}$, respectively. The $\mathbb{Z}_{\mathcal{N}}$ toric code Hamiltonian [62–64] is then

$$H_{\mathrm{DV}}^{\mathrm{tor}} := -\frac{J_z}{2} \sum_{\square} \left(\boldsymbol{Z}_{\raisebox{-1pt}{\tiny■}}^{\mathcal{M}} \boldsymbol{Z}_{\raisebox{-1pt}{\tiny■}}^{\mathcal{M}} \boldsymbol{Z}_{\raisebox{-1pt}{\tiny■}}^{-\mathcal{M}} \boldsymbol{Z}_{\raisebox{-1pt}{\tiny■}}^{-\mathcal{M}} + H.c. \right) - \frac{J_x}{2} \sum_{+} \left(\boldsymbol{X}_{\raisebox{-1pt}{\tiny+}}^{\mathcal{L}} \boldsymbol{X}_{\raisebox{-1pt}{\tiny+}}^{\mathcal{L}} \boldsymbol{X}_{\raisebox{-1pt}{\tiny+}}^{-\mathcal{L}} \boldsymbol{X}_{\raisebox{-1pt}{\tiny+}}^{-\mathcal{L}} + H.c. \right) \tag{74a}$$

$$= -J_z \sum_{\square} \cos\left(\frac{2\pi\mathcal{M}}{\mathcal{N}} \boldsymbol{s}_{\square} \right) - J_x \sum_{+} \cos\left(\frac{2\pi\mathcal{L}}{\mathcal{N}} \boldsymbol{m}_{+} \right), \tag{74b}$$

where $J_{x,z} > 0$ and $0 < \mathcal{M}, \mathcal{L} < \mathcal{N}$ are the hopping length scales for the respective variables. The joint degrees of freedom associated with *going around* a plaquette □ counterclockwise and *going out* of a vertex +, respectively, are

$$\boldsymbol{s}_{\square} = \boldsymbol{s}_{\raisebox{-1pt}{\tiny■}} + \boldsymbol{s}_{\raisebox{-1pt}{\tiny■}} - \boldsymbol{s}_{\raisebox{-1pt}{\tiny■}} - \boldsymbol{s}_{\raisebox{-1pt}{\tiny■}} \qquad \text{and} \qquad \boldsymbol{m}_{+} = \boldsymbol{m}_{\raisebox{-1pt}{\tiny+}} + \boldsymbol{m}_{\raisebox{-1pt}{\tiny+}} - \boldsymbol{m}_{\raisebox{-1pt}{\tiny+}} - \boldsymbol{m}_{\raisebox{-1pt}{\tiny+}}. \tag{75}$$

(Note how the $\mathcal{N} = 2$ case reduces to the original toric code.) The minus signs in $\boldsymbol{s}_{\square}, \boldsymbol{m}_{+}$ give the model an orientation [103] and make sure that all terms in $H_{\mathrm{DV}}^{\mathrm{tor}}$ commute with each other, meaning that $H_{\mathrm{DV}}^{\mathrm{tor}}$ is *frustration-free*. In the language of $\mathbb{Z}_{\mathcal{N}}$ gauge theory [62], $\boldsymbol{s}_{\square}$ is the magnetic field through □ while $\boldsymbol{m}_{+}$ is the electric charge at +.

Fixing $\mathcal{M} = \mathcal{L} = 1$ for this paragraph, the ground state is one for which $\boldsymbol{s}_{\square} = \boldsymbol{m}_{+} = 0$ (modulo $\mathcal{N}$) for all □ and +, respectively, and its lowest-energy excitations have $\boldsymbol{s}_{\square} = \pm 1$ or $\boldsymbol{m}_{+} = \pm 1$ for one □ or +. There exist four types of string-like conserved quantities which determine the ground-state degeneracy,

$$\boldsymbol{Z}_{\leftrightarrow} = \cdots \boldsymbol{Z}_{\raisebox{-1pt}{\tiny+}} \boldsymbol{Z}_{\raisebox{-1pt}{\tiny+}} \cdots, \qquad \boldsymbol{Z}_{\updownarrow} = \cdots \boldsymbol{Z}_{\raisebox{-1pt}{\tiny+}} \boldsymbol{Z}_{\raisebox{-1pt}{\tiny+}} \cdots, \qquad \boldsymbol{X}_{\leftrightarrow} = \cdots \boldsymbol{X}_{\raisebox{-1pt}{\tiny■}} \boldsymbol{X}_{\raisebox{-1pt}{\tiny■}} \cdots, \qquad \boldsymbol{X}_{\updownarrow} = \cdots \boldsymbol{X}_{\raisebox{-1pt}{\tiny■}} \boldsymbol{X}_{\raisebox{-1pt}{\tiny■}} \cdots, \tag{76a}$$

where the product is over all sites along either one of the two noncontractible loops of the torus. These satisfy $\boldsymbol{X}_{\leftrightarrow} \boldsymbol{Z}_{\updownarrow} \boldsymbol{X}_{\leftrightarrow}^{-1} \boldsymbol{Z}_{\updownarrow}^{-1} = \boldsymbol{X}_{\updownarrow} \boldsymbol{Z}_{\leftrightarrow} \boldsymbol{X}_{\updownarrow}^{-1} \boldsymbol{Z}_{\leftrightarrow}^{-1} = e^{-i\frac{2\pi}{\mathcal{N}}}$, implying that there is an $\mathcal{N}^2$-dimensional ground-state subspace that can be characterized by eigenvalues of

$$\boldsymbol{s}_{\leftrightarrow} = \cdots + \boldsymbol{s}_{\raisebox{-1pt}{\tiny+}} + \boldsymbol{s}_{\raisebox{-1pt}{\tiny+}} + \cdots \mod \mathcal{N} \qquad \text{and} \qquad \boldsymbol{s}_{\updownarrow} = \cdots + \boldsymbol{s}_{\raisebox{-1pt}{\tiny+}} + \boldsymbol{s}_{\raisebox{-1pt}{\tiny+}} + \cdots \mod \mathcal{N}. \tag{77}$$

Once again, we have introduced the $\mathcal{M}, \mathcal{L}$ degrees of freedom only to perform the DV → ROT and ROT → CV limits; they are not required for the direct DV → CV limit. Assuming $J_x \approx J_z$ and performing the DV → CV limit from Sec. III A yields, up to constant offsets and factors, the coupled-oscillator Hamiltonian

$$H_{\mathrm{CV}}^{\mathrm{tor}} := \frac{J_z}{2} \sum_{\square} \boldsymbol{p}_{\square}^2 + \frac{J_x}{2} \sum_{+} \boldsymbol{x}_{+}^2, \tag{78}$$

where $\boldsymbol{p}_{\square} = \boldsymbol{p}_{\raisebox{-1pt}{\tiny■}} + \boldsymbol{p}_{\raisebox{-1pt}{\tiny■}} - \boldsymbol{p}_{\raisebox{-1pt}{\tiny■}} - \boldsymbol{p}_{\raisebox{-1pt}{\tiny■}}$ and $\boldsymbol{x}_{+} = \boldsymbol{x}_{\raisebox{-1pt}{\tiny+}} + \boldsymbol{x}_{\raisebox{-1pt}{\tiny+}} - \boldsymbol{x}_{\raisebox{-1pt}{\tiny+}} - \boldsymbol{x}_{\raisebox{-1pt}{\tiny+}}$. This is exactly the Hamiltonian whose ground states are those of the CV surface code [65]. While this Hamiltonian was known before [104], the DV → CV limit-taking procedure provides its direct derivation from the original toric code. This system has an infinite-dimensional degeneracy [$\boldsymbol{s} \to \boldsymbol{p}$ in Eq. (77)] and is gapless.

While the direct DV → CV limit reproduces a known instance of the toric code, taking the ROT detour introduces two new generalizations. Performing the DV → ROT1, 2 limits from Sec. III B yields the respective coupled-rotor systems

$$H_{\mathrm{ROT1}}^{\mathrm{tor}} := -J_z \sum_{\square} \cos\left(2\pi\Phi\boldsymbol{N}_{\square} \right) - J_x \sum_{+} \cos\left(\mathcal{L}\boldsymbol{\theta}_{+} \right) \tag{79}$$

$$H_{\mathrm{ROT2}}^{\mathrm{tor}} := -J_z \sum_{\square} \cos\left(\mathcal{M}\boldsymbol{\theta}_{\square} \right) - J_x \sum_{+} \cos\left(2\pi\Phi\boldsymbol{N}_{+} \right). \tag{80}$$

The plaquette and vertex structure is of course preserved, but now the degree of freedom on each site is a rotor (ROT). The degrees of freedom of these models resemble those of compact $U(1)$ lattice gauge theory (LGT): $\boldsymbol{\theta}_{\square}$ is the magnetic flux term Φ in the equation below Eq. (6.4.13) in Ref. [45] while $\boldsymbol{N}_{+}$ can be interpreted as the electric charge at the center of the "+". In fact, the relation between $H_{\mathrm{ROT}}^{\mathrm{tor}}$ and $U(1)$ LGT is the same as that between $H_{\mathrm{DV}}^{\mathrm{tor}}$ and $\mathbb{Z}_{\mathcal{N}}$ LGT [62]: the H^{tor} systems consist of the flux term from their corresponding LGT along with a term which represents a local gauge transformation and whose value is constant within the ground-state subspace. Given that $U(1)$ gauge theory is always confined in two dimensions, it remains to be seen whether the rotor models can admit novel deconfined phases.

VIII. HAAH CUBIC CODE

The cubic code [66] is a three-dimensional generalization of the toric code and is an example of fracton topological order [105]. It is defined on a cubic lattice, where each site contains *two* DV($\mathcal{N} = 2$) subsystems. We denote the lattice cubes by $⊞$ and operators O acting nontrivially on the first ("•") or second ("×") subsystem on a given cube as, e.g., $O_{⊞}$ or $O_{⊞}$. The original Hamiltonian is

$$H_{\mathcal{N}=2}^{\mathrm{cub}} := -J_z \sum_{⊞} A_{⊞} - J_x \sum_{⊞} B_{⊞}, \tag{81}$$

where $J_{A,B} > 0$ and the sum is over all cubes in the lattice. The operators $A_{⊞}, B_{⊞}$ act nontrivially on 8 out of the 16 sites of the cube; we will not define them for conciseness and instead directly write the generalized DV($\mathcal{N} \geq 2$) version. Using the same tricks as for the toric code regarding defining an orientation and making sure all cubes commute [103], one can come up with the model

$$H_{\mathrm{DV}}^{\mathrm{cub}} := -\frac{J_z}{2} \sum_{⊞} \left(\boldsymbol{Z}_{⊞}^{\mathcal{M}} \boldsymbol{Z}_{⊞}^{\mathcal{M}} \boldsymbol{Z}_{⊞}^{\mathcal{M}} \boldsymbol{Z}_{⊞}^{\mathcal{M}} \boldsymbol{Z}_{⊞}^{\mathcal{M}} \boldsymbol{Z}_{⊞}^{\mathcal{M}} \boldsymbol{Z}_{⊞}^{\mathcal{M}} \boldsymbol{Z}_{⊞}^{\mathcal{M}} + H.c. \right) - \frac{J_x}{2} \sum_{⊞} \left(\boldsymbol{X}_{⊞}^{\mathcal{L}} \boldsymbol{X}_{⊞}^{\mathcal{L}} \boldsymbol{X}_{⊞}^{\mathcal{L}} \boldsymbol{X}_{⊞}^{\mathcal{L}} \boldsymbol{X}_{⊞}^{-\mathcal{L}} \boldsymbol{X}_{⊞}^{-\mathcal{L}} \boldsymbol{X}_{⊞}^{-\mathcal{L}} \boldsymbol{X}_{⊞}^{-\mathcal{L}} + H.c. \right)$$
$$= -J_z \sum_{⊞} \cos\left(\frac{2\pi\mathcal{M}}{\mathcal{N}} \left[\boldsymbol{s}_{⊞} + \boldsymbol{s}_{⊞} \right] \right) - J_x \sum_{⊞} \cos\left(\frac{2\pi\mathcal{L}}{\mathcal{N}} \left[\boldsymbol{m}_{⊞} - \boldsymbol{m}_{⊞} \right] \right), \tag{82}$$

where the first line is written in terms of Weyl operators (23a-23b) and the second in terms of their corresponding conjugate variables $\boldsymbol{s}, \boldsymbol{m}$ (18). The composite variables are, e.g., $\boldsymbol{s}_{⊞} = \boldsymbol{s}_{⊞} + \boldsymbol{s}_{⊞} + \boldsymbol{s}_{⊞} + \boldsymbol{s}_{⊞}$, with the remaining three defined similarly. The relative minus in the J_x-term is so that $H_{\mathrm{DV}}^{\mathrm{cub}}$ is frustration free. To verify this, one needs make sure that a given cube commutes with all of the 26 neighboring cubes with which it shares faces, sides, and corners. We further assume $J_x \approx J_z$ in order to further justify the DV → CV procedure. A simpler model can be defined with $\mathcal{M}, \mathcal{L} = 1$, but we do not assume this in order to more conveniently take all of the desired limits.

Performing the DV → CV limit from Sec. III A yields, up to constant offsets and factors, the coupled-oscillator Hamiltonian

$$H_{\mathrm{CV}}^{\mathrm{cub}} := \frac{1}{2} \sum_{⊞} \left(\boldsymbol{p}_{⊞} + \boldsymbol{p}_{⊞} \right)^2 + \frac{1}{2} \sum_{⊞} \left(\boldsymbol{x}_{⊞} - \boldsymbol{x}_{⊞} \right)^2. \tag{83}$$

Performing the DV → ROT1, 2 limits from Sec. III B yields the respective coupled-rotor systems

$$H_{\mathrm{ROT1}}^{\mathrm{cub}} := -\sum_{⊞} \cos\left(2\pi\Phi \left[\boldsymbol{N}_{⊞} + \boldsymbol{N}_{⊞} \right] \right) - \sum_{⊞} \cos\left(\mathcal{L} \left[\boldsymbol{\theta}_{⊞} - \boldsymbol{\theta}_{⊞} \right] \right) \tag{84}$$

$$H_{\mathrm{ROT2}}^{\mathrm{cub}} := -\sum_{⊞} \cos\left(\mathcal{M} \left[\boldsymbol{\theta}_{⊞} + \boldsymbol{\theta}_{⊞} \right] \right) - \sum_{⊞} \cos\left(2\pi\Phi \left[\boldsymbol{N}_{⊞} - \boldsymbol{N}_{⊞} \right] \right). \tag{85}$$

Note that the $\Phi \ll 1$ version of this model, in which one of the cosines is expanded, was independently written down and studied by Haah [106]. Since $U(1)$ lattice gauge theory can be deconfined in three dimensions [45], it will be interesting to examine whether these models can also admit interesting deconfined phases. All Hamiltonians remain frustration-free as that algebraic structure is preserved in this limit. We have thus generalized the $\mathcal{N} = 2$ cubic code to arbitrary $\mathcal{N}$ as well as to the ROT and CV phase spaces. Moreover, this recipe can be applied to any qudit stabilizer code.

IX. KITAEV HONEYCOMB MODEL

The Kitaev honeycomb model [67] is a two-dimensional exactly solvable model with an extensive number of conserved quantities that, along with its relative the toric code (see Sec. VII), is a paradigmatic model lying at the intersection of topological quantum phases of matter and quantum computation. It was originally defined on a honeycomb lattice; we denote the lattice plaquettes by $⬡$ and operators O on a given site "•" on a plaquette as, e.g., $O_{⬡}$ or $O_{⬡}$. The original model is defined on a set of DV($\mathcal{N} = 2$) sites, but has been extended to lattices consisting of sites of the type DV for arbitrary $\mathcal{N}$ [68, 69] (see [107] for a different extension). We write such a model below

in terms of Weyl operators (23a-23b), using the convention of Ref. [68] but adding the hopping length scales $\mathcal{M}, \mathcal{L}$ in order to more conveniently take all of the limits we desire:

$$H_{\mathrm{DV}}^{\mathrm{hon}} = -\frac{1}{2} \sum_{\hexagon} \left(J_x \boldsymbol{X}^{\mathcal{L}} \boldsymbol{X}^{\mathcal{L}} + J_y \boldsymbol{Y}^{\mathcal{M},\mathcal{L}} \boldsymbol{Y}^{\mathcal{M},\mathcal{L}} + J_z \boldsymbol{Z}^{\mathcal{M}} \boldsymbol{Z}^{\mathcal{M}} + H.c. \right), \tag{86}$$

where $J_{x,y,z} > 0$, $\boldsymbol{Y} = \boldsymbol{Z}^{-1}\boldsymbol{X}^{-1}$, and $\boldsymbol{Y}^{\mathcal{M},\mathcal{L}} = \boldsymbol{Z}^{-\mathcal{M}}\boldsymbol{X}^{-\mathcal{L}}$. In terms of the conjugate variables $\boldsymbol{s}, \boldsymbol{m}$ (18), we have

$$H_{\mathrm{DV}}^{\mathrm{hon}} = -J_x \sum_{\hexagon} \cos\left(\frac{2\pi\mathcal{L}}{\mathcal{N}}\left[\boldsymbol{m} + \boldsymbol{m}\right]\right) - J_z \sum_{\hexagon} \cos\left(\frac{2\pi\mathcal{M}}{\mathcal{N}}\left[\boldsymbol{s} + \boldsymbol{s}\right]\right) \tag{87}$$

$$-J_y \sum_{\hexagon} \left(\exp\left[-i\frac{2\pi\mathcal{M}}{\mathcal{N}}\left\{\boldsymbol{s} + \boldsymbol{s}\right\}\right]\exp\left[i\frac{2\pi\mathcal{L}}{\mathcal{N}}\left\{\boldsymbol{m} + \boldsymbol{m}\right\}\right] + H.c.\right).$$

This model has a conserved quantity for each plaquette,

$$W_{\mathrm{DV}}^{\hexagon} = \boldsymbol{Y}\,\boldsymbol{Z}\,\boldsymbol{X}\,\boldsymbol{Y}\,\boldsymbol{Z}\,\boldsymbol{X} = \exp\left(-i\frac{2\pi\mathcal{M}}{\mathcal{N}}\left[\boldsymbol{s} - \boldsymbol{s} + \boldsymbol{s} - \boldsymbol{s}\right]\right)\exp\left(i\frac{2\pi\mathcal{L}}{\mathcal{N}}\left[\boldsymbol{m} - \boldsymbol{m} + \boldsymbol{m} - \boldsymbol{m}\right]\right), \tag{88}$$

where the $\mathcal{M}, \mathcal{L}$ factors are necessary for $W_{\mathrm{DV}}^{\hexagon}$ to commute with the J_y-term. There are also conserved quantities consisting of Weyl operators along any horizontal or 60-degree zig-zag of the lattice,

$$V_{\mathrm{DV}}^{\leftrightarrow} = \cdots \boldsymbol{X}^{-1}\boldsymbol{X}\,\boldsymbol{X}^{-1}\cdots = \exp\left(-\frac{2\pi}{\mathcal{N}}\left[\cdots\boldsymbol{m} - \boldsymbol{m} + \boldsymbol{m}\cdots\right]\right) \tag{89a}$$

$$V_{\mathrm{DV}}^{\nearrow} = \cdots \boldsymbol{Z}\,\boldsymbol{Z}^{-1}\boldsymbol{Z}\cdots = \exp\left(\frac{2\pi}{\mathcal{N}}\left[\cdots\boldsymbol{s} - \boldsymbol{s} + \boldsymbol{s}\cdots\right]\right). \tag{89b}$$

We have $V_{\mathrm{DV}}^{\leftrightarrow} V_{\mathrm{DV}}^{\nearrow} = e^{-i\frac{4\pi}{N}} V_{\mathrm{DV}}^{\nearrow} V_{\mathrm{DV}}^{\leftrightarrow}$, implying a non-trivial ground-state degeneracy of the model on the torus [68]. Unlike the toric code, this model is not frustration-free and exhibits different phases for different values of the parameters. We expand around the symmetric case $J_x \approx J_y \approx J_z$, for which the $\mathcal{N} = 2, \mathcal{M} = \mathcal{L} = 1$ system is known to be gapless [67].

Performing the DV → CV limit from Sec. III A yields the coupled-oscillator Hamiltonian

$$H_{\mathrm{CV}}^{\mathrm{hon}} := \sum_{\hexagon} J_x\left(\boldsymbol{x} + \boldsymbol{x}\right)^2 + J_y\left(\boldsymbol{p} - \boldsymbol{x} + \boldsymbol{p} - \boldsymbol{x}\right)^2 + J_z\left(\boldsymbol{p} + \boldsymbol{p}\right)^2. \tag{90}$$

All conserved quantities are preserved: for each plaquette,

$$W_{\mathrm{CV}}^{\hexagon} = \boldsymbol{p} - \boldsymbol{x} - \boldsymbol{p} + \boldsymbol{x} + \boldsymbol{p} - \boldsymbol{x} - \boldsymbol{p} + \boldsymbol{x}, \tag{91}$$

and the string operators are

$$V_{\mathrm{CV}}^{\nearrow} = \cdots\boldsymbol{p} - \boldsymbol{p} + \boldsymbol{p}\cdots \qquad \text{and} \qquad V_{\mathrm{DV}}^{\leftrightarrow} = \cdots\boldsymbol{x} - \boldsymbol{x} + \boldsymbol{x}\cdots. \tag{92}$$

The string operators satisfy $[V_{\mathrm{DV}}^{\leftrightarrow}, V_{\mathrm{DV}}^{\nearrow}] = -2i$, meaning that the ground-state degeneracy on a torus is infinite (since there are no finite-dimensional irreducible representations of the Heisenberg-Weyl algebra).

Performing the DV → ROT1 limit from Sec. III B yields the coupled-rotor system

$$H_{\mathrm{ROT1}} = -J_x \sum_{\hexagon} \cos\left(\mathcal{L}\left[\boldsymbol{\theta} + \boldsymbol{\theta}\right]\right) - J_z \sum_{\hexagon} \cos\left(2\pi\Phi\left[\boldsymbol{N} + \boldsymbol{N}\right]\right) \tag{93}$$

$$-\frac{J_y}{2} \sum_{\hexagon} \left(\exp\left[-i2\pi\Phi\left\{\boldsymbol{N} + \boldsymbol{N}\right\}\right]\exp\left[i\mathcal{L}\left\{\boldsymbol{\theta} + \boldsymbol{\theta}\right\}\right] + H.c.\right).$$

The conserved quantities turn into plaquette operators

$$W_{\mathrm{ROT1}} = \exp\left(-i2\pi\Phi\left[\boldsymbol{N} - \boldsymbol{N} + \boldsymbol{N} - \boldsymbol{N}\right]\right)\exp\left(i\mathcal{L}\left[\boldsymbol{\theta} - \boldsymbol{\theta} + \boldsymbol{\theta} - \boldsymbol{\theta}\right]\right) \tag{94}$$

and string operator generators

$$V_{\mathrm{ROT1}}^{\nearrow} = \cdots\boldsymbol{N} - \boldsymbol{N} + \boldsymbol{N}\cdots \qquad \text{and} \qquad V_{\mathrm{ROT1}}^{\leftrightarrow} = \cdots\boldsymbol{\theta} - \boldsymbol{\theta} + \boldsymbol{\theta}\cdots. \tag{95}$$

The limit DV → ROT2 is equivalent to this limit upon $J_x \leftrightarrow J_z$ and a reflection.

X. SUMMARY AND OUTLOOK

The first part of this work provides an introduction to three types of phase spaces whose conjugate variables can be related via a Fourier-type transformation. The first type (DV) involves two discrete finite conjugate variables $\{s, m\}$, the second type (ROT) involves an integer-valued variable and its conjugate angle $\{N, \theta\}$, and the last type (CV) is ordinary phase space of two continuous conjugate variables $\{x, p\}$. The second part of this work is concerned with converting Hamiltonians living in one phase space into those in the others (DV → CV, DV → ROT, and ROT → CV). These limit-taking procedures correspond directly to the limits connecting functions of a discrete periodic variable (DV) to those of a continuous periodic variable (ROT) or those of an unbounded variable (CV) (Secs. 3.4.2 and 3.4.5 of Ref. [38], respectively). We outlined slightly generalized versions of these well-known procedures and applied them to the DV degrees of freedom in six models: the Harper equation, the Baxter parafermionic spin chain, the Rabi model, the toric code, the Haah cubic code, and the Kitaev honeycomb model. Interestingly, these straightforward limit-taking procedures resulted in rotor and continuum limits for all six models, making contact with the quantum Hall effect, optomechanics, and lattice gauge theory. We hope these new models will be studied further and that these techniques will be useful in generating interesting new rotor and continuum limits. In particular, it would be interesting to rigorously determine whether spectra of the DV models converge to their CV limits (as opposed to the CV limit being merely a low-energy expansion). This has so far only been done for the oscillator, but the solvability of most of the systems considered [58, 62, 66, 67, 108] makes this direction quite promising.

We conclude with an outlook regarding experimental realizations. For the Rabi model, implementation of the $\mathcal{N} \gg 1$ circular structure is admittedly tricky, as one has to engineer equal transition amplitudes for all sites and also ensure that photons are either absorbed or emitted, depending on the direction of the hopping. However, it is not improbable that one can find a proper multi-level artificial atom based on superconducting circuits whose transition rules satisfy the $\mathcal{N} = 3$ or even $\mathcal{N} = 4$ Rabi models. The optimal candidate for realizing high $\mathcal{N}$ cases however is optical lattices [109] or trapped ions [110–112], where ring-shaped potentials can already be engineered. Similar experimental platforms have been proposed to simulate $\mathbb{Z}_\mathcal{N}$ lattice gauge theories [113]. For the many-body coupled rotor models, one could consider engineering interactions between orbital angular momentum degrees of freedom of photonic modes (e.g., [114, 115]).

[1] A. Auerbach, *Interacting Electrons and Quantum Magnetism* (Springer-Verlag, New York, 1994).

[2] A. Vourdas, *Finite and Profinite Quantum Systems*, Quantum Science and Technology (Springer International Publishing, Cham, 2017).

[3] R. F. Werner, *Uncertainty relations for general phase spaces*, Front. Phys. **11**, 110305 (2016).

[4] R. Lenz, *Group Theoretical Methods in Image Processing*, Lecture Notes in Computer Science, Vol. 413 (Springer Berlin Heidelberg, Berlin, Heidelberg, 1990) p. 75.

[5] N. Cotfas and D. Dragoman, *Properties of finite Gaussians and the discrete-continuous transition*, J. Phys. A: Math. Theor. **45**, 425305 (2012).

[6] R. Gilmore, *Lie groups, Lie algebras, and some of their applications* (Dover Publications, New York, 1974) p. 428.

[7] A. Klein and E. R. Marshalek, *Boson realizations of Lie algebras with applications to nuclear physics*, Rev. Mod. Phys. **63**, 375 (1991).

[8] T. Durt, B.-G. Englert, I. Bengtsson, and K. Zyczkowski, *On mutually unbiased bases*, Int. J. Quantum Inf. **08**, 535 (2010).

[9] J. J. Sylvester, *The collected mathematics papers of James Joseph Sylvester* (Cambridge University Press, Cambridge, 1909).

[10] J. von Neumann, *Die Eindeutigkeit der Schrödingerschen Operatoren*, Math. Ann. **104**, 570 (1931).

[11] H. Weyl, *The theory of groups and quantum mechanics*, 2nd ed. (Dover, USA, 1950) p. 272.

[12] J. Schwinger, *Quantum Kinematics and Dynamics* (Westview Press, Boulder, 2000).

[13] D. Gottesman, A. Yu. Kitaev, and J. Preskill, *Encoding a qubit in an oscillator*, Phys. Rev. A **64**, 012310 (2001).

[14] A. Pittenger and M. H. Rubin, *Mutually unbiased bases, generalized spin matrices and separability*, Linear Algebra Appl. **390**, 255 (2004).

[15] M. R. Kibler, *An angular momentum approach to quadratic Fourier transform, Hadamard matrices, Gauss sums, mutually unbiased bases, the unitary group and the Pauli group,* J. Phys. A: Math. Theor. **42**, 353001 (2009).

[16] C. Sachse, *Sylvester-'t Hooft generators and relations between them for sl(n) and gl(n/n),* Theor. Math. Phys. **149**, 1299 (2006).

[17] G. Landi, F. Lizzi, and R. J. Szabo, *From Large N Matrices to the Noncommutative Torus,* Commun. Math. Phys. **217**, 181 (2001).

[18] B. C. Hall, *Quantum Theory for Mathematicians*, Graduate Texts in Mathematics, Vol. 267 (Springer New York, New York, NY, 2013).

[19] D. Galetti and M. Marchiolli, *Discrete Coherent States and Probability Distributions in Finite-Dimensional Spaces,* Ann. Phys. **249**, 454 (1996).

[20] M. Ruzzi, M. A. Marchiolli, and D. Galetti, *Extended Cahill-Glauber formalism for finite-dimensional spaces: I. Fundamentals,* J. Phys. A: Math. Gen. **38**, 6239 (2005).

[21] M. A. Marchiolli, M. Ruzzi, and D. Galetti, *Discrete squeezed states for finite-dimensional spaces,* Phys. Rev. A **76**, 032102 (2007).

[22] A. Ketkar, A. Klappenecker, S. Kumar, and P. Sarvepalli, *Nonbinary Stabilizer Codes Over Finite Fields,* IEEE Trans. Inf. Theory **52**, 4892 (2006).

[23] D. Galetti and A. de Toledo Piza, *An extended Weyl-Wigner transformation for special finite spaces,* Physica A **149**, 267 (1988).

[24] M. Ruzzi and D. Galetti, *Quantum discrete phase space dynamics and its continuous limit,* J. Phys. A: Math. Gen. **33**, 1065 (2000).

[25] K. S. Gibbons, M. J. Hoffman, and W. K. Wootters, *Discrete phase space based on finite fields,* Phys. Rev. A **70**, 062101 (2004).

[26] M. A. Marchiolli, M. Ruzzi, and D. Galetti, *Extended Cahill-Glauber formalism for finite-dimensional spaces. II. Applications in quantum tomography and quantum teleportation,* Phys. Rev. A **72**, 042308 (2005).

[27] C. Ferrie, *Quasi-probability representations of quantum theory with applications to quantum information science,* Rep. Prog. Phys. **74**, 116001 (2011).

[28] M. Marchiolli and M. Ruzzi, *Theoretical formulation of finite-dimensional discrete phase spaces: I. Algebraic structures and uncertainty principles,* Ann. Phys. **327**, 1538 (2012).

[29] T. Tilma, M. J. Everitt, J. H. Samson, W. J. Munro, and K. Nemoto, *Wigner Functions for Arbitrary Quantum Systems,* Phys. Rev. Lett. **117**, 180401 (2016).

[30] M. Ligabò, *Torus as phase space: Weyl quantization, dequantization, and Wigner formalism,* J. Math. Phys. **57**, 082110 (2016).

[31] A. Miranowicz and N. Imoto, in *Modern nonlinear optics, part I* (John Wiley & Sons, New York, 2001) p. 195.

[32] A. C. de la Torre and D. Goyeneche, *Quantum mechanics in finite-dimensional Hilbert space,* Am. J. Phys. **71**, 49 (2003).

[33] I. Bengtsson and K. Zyczkowski, *On discrete structures in finite Hilbert spaces,* arXiv:1701.07902.

[34] L. I. Schiff, *Quantum Mechanics* (McGraw-Hill Book Company, New York, 1968).

[35] R. R. Puri, *Mathematical methods of quantum optics* (Springer, Berlin/Heidelberg, 2001).

[36] F. T. Arecchi, E. Courtens, R. Gilmore, and H. Thomas, *Atomic Coherent States in Quantum Optics,* Phys. Rev. A **6**, 2211 (1972).

[37] N. M. Atakishiyev, G. S. Pogosyan, and K. B. Wolf, *Contraction of the finite one-dimensional oscillator,* Int. J. Mod. Phys. A **18**, 317 (2003).

[38] K. B. Wolf, *Integral transforms in science and engineering* (Plenum Press, New York, 1979).

[39] K. Kowalski, J. Rembielinski, and L. C. Papaloucas, *Coherent states for a quantum particle on a circle,* J. Phys. A: Math. Gen. **29**, 4149 (1996).

[40] M. V. Berry, *Semi-Classical Mechanics in Phase Space: A Study of Wigner's Function,* Philos. T. Roy. Soc. A **287** (1977).

[41] N. Mukunda, *Wigner distribution for angle coordinates in quantum mechanics,* Am. J. Phys. **47**, 182 (1979).

[42] S. Zhang and A. Vourdas, *Phase space methods for particles on a circle,* J. Math. Phys. **44**, 5084 (2003).

[43] M. Ruzzi, M. A. Marchiolli, E. C. da Silva, and D. Galetti, *Quasiprobability distribution functions for periodic phase spaces: I. Theoretical aspects,* J. Phys. A: Math. Gen. **39**, 9881 (2006).

[44] P. Raynal, A. Kalev, J. Suzuki, and B.-G. Englert, *Encoding many qubits in a rotor,* Phys. Rev. A **81**, 052327 (2010).

[45] X.-g. Wen, *Quantum field theory of many-body systems* (Oxford University Press, Oxford, 2004).

[46] N. W. Ashcroft and N. D. Mermin, *Solid state physics*, 1st ed. (Harcourt College Publishers, Fort Worth, 1976).

[47] S. M. Girvin, in *Quantum machines: measurement and control of engineered quantum systems*, edited by M. H. Devoret, B. Huard, R. J. Schoelkopf, and L. F. Cugliandolo (Oxford University Press, Oxford, 2015) Chap. 3.

[48] M. H. Devoret, in *Quantum fluctuations*, edited by S. Reynaud, E. Giacobino, and J. Zinn-Justin (Elsevier, Amsterdam, 1997) Chap. 10.

[49] M. Ruzzi, *Schwinger, Pegg and Barnett approaches and a relationship between angular and Cartesian quantum descriptions,* J. Phys. A: Math. Gen. **35**, 1763 (2002).

[50] M. Ruzzi and D. Galetti, *Schwinger and Pegg-Barnett approaches and a relationship between angular and Cartesian quantum descriptions: II. Phase spaces,* J. Phys. A: Math. Gen. **35**, 4633 (2002).

[51] S. Haroche and J.-M. Raimond, *Exploring the quantum: atoms, cavities, and photons* (Oxford University Press, Oxford, 2006).

[52] J. C. Garrison and J. Wong, *Canonically Conjugate Pairs, Uncertainty Relations, and Phase Operators,* J. Math. Phys. **11**, 2242 (1970).
[53] R. Lynch, *The quantum phase problem: a critical review,* Physics Reports **256**, 367 (1995).
[54] W. P. Schleich, *Quantum optics in phase space* (Wiley, Berlin, 2001).
[55] M. Y. Azbel, *Energy spectrum of a conduction electron in a magnetic field,* J. Exp. Theor. Phys. **19**, 634 (1964).
[56] D. Hofstadter, *Energy levels and wave functions of Bloch electrons in rational and irrational magnetic fields,* Phys. Rev. B **14**, 2239 (1976).
[57] A. Avila and S. Jitomirskaya, *The Ten Martini Problem,* Ann. Math. **170**, 303 (2009).
[58] R. Baxter, *A simple solvable ZN Hamiltonian,* Phys. Lett. A **140**, 155 (1989).
[59] I. I. Rabi, *On the Process of Space Quantization,* Phys. Rev. **49**, 324 (1936).
[60] I. I. Rabi, *Space Quantization in a Gyrating Magnetic Field,* Phys. Rev. **51**, 652 (1937).
[61] V. V. Albert, *Quantum Rabi Model for N-State Atoms,* Phys. Rev. Lett. **108**, 180401 (2012).
[62] A. Yu. Kitaev, *Fault-tolerant quantum computation by anyons,* Ann. Phys. **303**, 2 (2003).
[63] X.-G. Wen, *Quantum Orders in an Exact Soluble Model,* Phys. Rev. Lett. **90**, 016803 (2003).
[64] S. S. Bullock and G. K. Brennen, *Qudit surface codes and gauge theory with finite cyclic groups,* J. Phys. A: Math. Theor. **40**, 3481 (2007).
[65] J. Zhang, C. Xie, K. Peng, and P. van Loock, *Anyon statistics with continuous variables,* Phys. Rev. A **78**, 052121 (2008).
[66] J. Haah, *Local stabilizer codes in three dimensions without string logical operators,* Phys. Rev. A **83**, 042330 (2011).
[67] A. Yu. Kitaev, *Anyons in an exactly solved model and beyond,* Ann. Phys. **321**, 2 (2006).
[68] M. Barkeshli, H.-C. Jiang, R. Thomale, and X.-L. Qi, *Generalized Kitaev Models and Extrinsic Non-Abelian Twist Defects,* Phys. Rev. Lett. **114**, 026401 (2015).
[69] P. Fendley, *Parafermionic edge zero modes in Z n -invariant spin chains,* J. Stat. Mech. **2012**, P11020 (2012).
[70] L. Barker, *Continuum Quantum Systems as Limits of Discrete Quantum Systems, I: State Vectors,* J. Funct. Anal. **186**, 153 (2001).
[71] L. Barker, *Continuum quantum systems as limits of discrete quantum systems: II. State functions,* J. Phys. A: Math. Gen. **34**, 4673 (2001).
[72] L. Barker, *Continuum quantum systems as limits of discrete quantum systems. III. Operators,* J. Math. Phys. **42**, 4653 (2001).
[73] L. Barker, *Continuum quantum systems as limits of discrete quantum systems. IV. Affine canonical transforms,* J. Math. Phys. **44**, 1535 (2003).
[74] T. Digernes, V. S. Varadarajan, and S. R. S. Varadhan, *Finite approximations to quantum systems,* Rev. Math. Phys. **06**, 621 (1994).
[75] S. Massar and P. Spindel, *Uncertainty Relation for the Discrete Fourier Transform,* Phys. Rev. Lett. **100**, 190401 (2008).
[76] L. Barker, C. Candanu, T. H. And, M. A. Kutay, and H. M. Ozaktas, *The discrete harmonic oscillator, Harper's equation, and the discrete fractional Fourier transform,* J. Phys. A: Math. Gen. **33**, 2209 (2000).
[77] L. Barker, *The discrete fractional Fourier transform and Harper's equation,* Mathematika **47**, 281 (2000).
[78] Y. Wang, B. Pannetier, and R. Rammal, *Quasiclassical approximations for almost-Mathieu equations,* J. Phys. Paris **48**, 2067 (1987).
[79] Y. E. Kraus and O. Zilberberg, *Topological Equivalence between the Fibonacci Quasicrystal and the Harper Model,* Phys. Rev. Lett. **109**, 116404 (2012).
[80] P. Fendley, *Free parafermions,* J. Phys. A: Math. Theor. **47**, 075001 (2014).
[81] F. C. Alcaraz, M. T. Batchelor, and Z.-Z. Liu, *Energy spectrum and critical exponents of the free parafermion Z N spin chain,* J. Phys. A: Math. Theor. **50**, 16LT03 (2017).
[82] J. Sólyom and P. Pfeuty, *Renormalization-group study of the Hamiltonian version of the Potts model,* Phys. Rev. B **24**, 218 (1981).
[83] A. Cant and P. A. Pearce, *Mean-field limits of the quantum Potts model,* Commun. Math. Phys. **90**, 373 (1983).
[84] A. Vaezi and E.-A. Kim, *UV-IR transmutation for hybrid realizations of Zk parafermion systems,* arXiv:1310.7434.
[85] N. Moran, D. Pellegrino, J. K. Slingerland, and G. Kells, *Parafermionic clock models and quantum resonance,* Phys. Rev. B **95**, 235127 (2017).
[86] M. E. Peskin, *Mandelstam-'t Hooft duality in abelian lattice models,* Ann. Phys. **113**, 122 (1978).
[87] L. Capriotti, A. Cuccoli, A. Fubini, V. Tognetti, and R. Vaia, in *Fundamental Problems of Mesoscopic Physics* (Kluwer Academic Publishers, Dordrecht, 2004) pp. 203–216.
[88] E. T. Jaynes and F. W. Cummings, *Comparison of quantum and semiclassical radiation theories with application to the beam maser,* P. IEEE **51**, 89 (1963).
[89] H. Paul, *Induzierte Emission bei starker Einstrahlung,* Ann. Phys. (Berlin) **466**, 411 (1963).
[90] B. W. Shore and P. L. Knight, *The Jaynes-Cummings model,* J. Mod. Optic. **40**, 1195 (1993).
[91] M. Lewenstein, A. Kubasiak, J. Larson, C. Menotti, G. Morigi, K. Osterloh, and A. Sanpera, in *AIP Conf. Proc.*, Vol. 869 (AIP, 2006) pp. 201–211.
[92] M. Tomka, M. Pletyukhov, and V. Gritsev, *Supersymmetry in quantum optics and in spin-orbit coupled systems,* Sci. Rep. **5**, 13097 (2015).
[93] B. A. Bernevig and S.-C. Zhang, *Quantum Spin Hall Effect,* Phys. Rev. Lett. **96**, 106802 (2006).
[94] I. H. Deutsch, P. M. Alsing, J. Grondalski, S. Ghose, D. L. Haycock, and P. S. Jessen, *Quantum transport in magneto-*

optical double-potential wells, J. Opt. B - Quantum S. O. **2**, 633 (2000).

[95] H. B. Shore and L. M. Sander, *Ground State of the Exciton-Phonon System,* Phys. Rev. B **7**, 4537 (1973).

[96] U. Herfort and M. Wagner, *Quantum dynamics of the prototype polaron model,* J. Phys.: Condens. Matter **13**, 3297 (2001).

[97] P. Rabl, P. Cappellaro, M. Dutt, L. Jiang, J. Maze, and M. D. Lukin, *Strong magnetic coupling between an electronic spin qubit and a mechanical resonator,* Phys. Rev. B **79**, 041302 (2009).

[98] E. R. MacQuarrie, T. A. Gosavi, N. R. Jungwirth, S. A. Bhave, and G. D. Fuchs, *Mechanical Spin Control of Nitrogen-Vacancy Centers in Diamond,* Phys. Rev. Lett. **111**, 227602 (2013).

[99] Y.-Z. Zhang, *symmetric chiral Rabi model: A new -level system,* Ann. Phys. **347**, 122 (2014).

[100] S. Ghose, P. M. Alsing, B. C. Sanders, and I. H. Deutsch, *Entanglement and the quantum-to-classical transition,* Phys. Rev. A **72**, 014102 (2005).

[101] L. Bakemeier, A. Alvermann, and H. Fehske, *Quantum phase transition in the Dicke model with critical and noncritical entanglement,* Phys. Rev. A **85**, 043821 (2012).

[102] R. Gilmore, *Catastrophe theory for scientists and engineers* (Dover Publications, New York, 1993).

[103] O. Viyuela, A. Rivas, and M. A. Martin-Delgado, *Generalized toric codes coupled to thermal baths,* New J. Phys. **14**, 033044 (2012).

[104] T. F. Demarie, T. Linjordet, N. C. Menicucci, and G. K. Brennen, *Detecting topological entanglement entropy in a lattice of quantum harmonic oscillators,* New J. Phys. **16**, 085011 (2014).

[105] S. Vijay, J. Haah, and L. Fu, *Fracton topological order, generalized lattice gauge theory, and duality,* Phys. Rev. B **94**, 235157 (2016).

[106] J. Haah, Two generalizations of the cubic code model,   (2013).

[107] A. Vaezi, *Z3 generalization of the Kitaev's spin-1/2 model,* Phys. Rev. B **90**, 075106 (2014).

[108] D. Braak, *Integrability of the Rabi Model,* Phys. Rev. Lett. **107**, 100401 (2011).

[109] L. Amico, A. Osterloh, and F. Cataliotti, *Quantum Many Particle Systems in Ring-Shaped Optical Lattices,* Phys. Rev. Lett. **95**, 063201 (2005).

[110] A. Noguchi, Y. Shikano, K. Toyoda, and S. Urabe, *Aharonov-Bohm effect in the tunnelling of a quantum rotor in a linear Paul trap,* Nat. Commun. **5**, 3868 (2014).

[111] B. Tabakov, F. Benito, M. Blain, C. R. Clark, S. Clark, R. A. Haltli, P. Maunz, J. D. Sterk, C. Tigges, and D. Stick, *Assembling a Ring-Shaped Crystal in a Microfabricated Surface Ion Trap,* Phys. Rev. Applied **4**, 031001 (2015).

[112] H.-K. Li, E. Urban, C. Noel, A. Chuang, Y. Xia, A. Ransford, B. Hemmerling, Y. Wang, T. Li, H. Häffner, and X. Zhang, *Realization of Translational Symmetry in Trapped Cold Ion Rings,* Phys. Rev. Lett. **118**, 053001 (2017).

[113] S. Notarnicola, E. Ercolessi, P. Facchi, G. Marmo, S. Pascazio, and F. V. Pepe, *Discrete Abelian gauge theories for quantum simulations of QED,* J. Phys. A: Math. Theor. **48**, 30FT01 (2015).

[114] A. I. Lvovsky, B. C. Sanders, and W. Tittel, *Optical quantum memory,* Nat. Photon. **3**, 706 (2009).

[115] A. Nicolas, L. Veissier, L. Giner, E. Giacobino, D. Maxein, and J. Laurat, *A quantum memory for orbital angular momentum photonic qubits,* Nat. Photon. **8**, 234 (2014).